Available online at www. jenams.com

Journal of Engineering and Management Studies

(E-ISSN: 2476-3055; ISSN: 2676-6957)

Vol. 2, No. 1, 019, 2026

A Review of Additive Manufacturing for Corrosion Control: Environmental Influences and Superhydrophobic Surface Development

***Abdurrezagh Mohamed Kazouz**

***Corresponding author: Abdurrezagh.Kazouz@cranfield.ac.uk**

Faculty of Engineering and Applied Science Cranfield University

Received: 09/09/2025; Accepted: 25/11/2025; Published: 01/03/2026

ABSTRACT:

Steel pipelines play a crucial role in transporting fluids across many industrial sectors. However, their long-term performance is often compromised by corrosion, particularly when buried in soils with acidic or alkaline properties. Corrosion not only weakens structural integrity but also increases the risk of leaks and system failures, leading to costly repairs and operational disruptions. While protective methods such as coatings, cathodic protection, and chemical inhibitors have been widely applied, they often fail when facing harsh environments, complex geometries or long-term use. In recent years, additive manufacturing (AM), also known as 3D printing, has opened new possibilities for corrosion prevention by allowing tailored material properties and surface designs. This review explores how AM technologies can complement and improve traditional protection strategies. It discusses corrosion mechanisms relevant to soil environments, reviews established and emerging prevention methods, and highlights how features like hydrophobic surface structuring and nanomaterial integration may enhance corrosion resistance. The potential for producing complex, application-specific protective solutions is also examined. Overall, this paper outlines a path forward where AM and materials engineering work together to develop more adaptable, effective and durable solutions for pipeline corrosion management.

Keywords: Corrosion protection, Environmental Influence, Polymers, 3D Printing, Hydrophobic Surface.

1. Introduction:

Corrosion remains one of the most persistent and technically challenging threats to the integrity and reliability of metallic infrastructure, particularly steel pipeline systems used for energy transport, chemical processing and water distribution networks *Adabavazeh et al., 2024)*. For buried and exposed pipelines, the severity of degradation depends on environmental complexity and the interaction between material, electrolyte availability, and transport processes within the surrounding medium. Fundamentally electrochemical, corrosion involves anodic metal dissolution coupled with cathodic reactions, with kinetics strongly influenced by pH, dissolved salts, oxygen availability, moisture and microbial activity, as well as operational variables such as temperature gradients and cyclic stresses *Kassinis et al., 2025*. In practical engineering terms, these conditions promote a spectrum of damage modes including general wall thinning, localized pitting corrosion, under-deposit corrosion and stress corrosion cracking, which may progress silently until leakage, rupture, or unacceptable loss of mechanical integrity occurs . Beyond direct structural consequences, corrosion-driven pipeline

failures are associated with substantial operational interruption, environmental contamination and costly rehabilitation, making corrosion control a central component of pipeline safety and life-cycle management. The economic implications of corrosion further emphasize the importance of robust prevention strategies. Global assessments estimate that the total cost of corrosion reaches over US$2 trillion annually, surpassing 3% of global GDP, while also highlighting that a meaningful fraction of this burden can be reduced through effective corrosion management and prevention practices]. These losses are not limited to direct replacement and repair costs, but extend to monitoring requirements, unplanned downtime, productivity reduction, safety risks, and environmental remediation. Although corrosion cannot be fully eliminated due to thermodynamic driving forces, the scale of its impact supports continued advancement of materials, coatings, and design approaches capable of extending service life, particularly for assets operating in aggressive environments.

Conventional corrosion control strategies for pipelines rely on combinations of barrier coatings, cathodic protection systems, inhibitors, and mechanical repair technologies, including composite wraps and localized patching. Polymeric coatings remain a dominant first-line defense due to their effectiveness in isolating steel from electrolytes, oxygen, and ionic species. Nevertheless, long-term performance is frequently compromised by coating defects, mechanical damage during installation or operation, aging phenomena, ultraviolet exposure for above-ground assets and chemical degradation in complex environments. Cathodic protection provides an additional protective layer by shifting electrochemical potentials, but its effectiveness depends on continuity, adequate electrical connectivity, proper current distribution and the presence of defects that may trigger localized corrosion and under-film attack.

In recent years, materials engineering has increasingly explored surface-functional solutions that go beyond passive barrier protection. Among these strategies, superhydrophobic coatings have gained attention due to their potential to reduce the residence time of aqueous electrolytes and minimize the effective contact area between water and metallic substrates, thereby limiting corrosion initiation and propagation. Superhydrophobic anticorrosion systems can operate through multiple protective mechanisms, including reduced wetting, decreased ion transport, delayed electrolyte penetration, and improved barrier stability under immersion and humid exposure conditions. However, the translation of laboratory superhydrophobic surfaces into field-relevant corrosion protection remains limited by durability challenges, such as mechanical abrasion, thermal aging, coating delamination and loss of hierarchical surface structures required to sustain extreme water repellency. These limitations are particularly critical for pipelines, where coatings must remain intact underground movement, handling, impact and long-term chemical exposure.

The performance of protective layers is also strongly influenced by environmental media, especially for underground pipelines where soil introduces complex corrosion drivers. Soil corrosion is governed not only by moisture availability, but also by ionic conductivity, chloride and sulfate concentrations, aeration gradients, pH variability, and time-dependent changes in local chemistry. Consequently, many corrosion investigations increasingly employ simulated soil solutions and electrochemical testing approaches to reproduce realistic pipeline exposure scenarios and quantify corrosion performance under accelerated yet representative conditions. In parallel with advances in functional coatings, additive manufacturing (AM) has emerged as a disruptive tool capable of redefining how anticorrosive surfaces are designed, fabricated, and tailored to application-specific geometries.

Despite these developments, the field still faces major scientific and technological questions.

The formation of super hydrophobicity is sensitive to both chemical composition and hierarchical surface morphology, yet AM introduces anisotropy, layer interfaces and scale-dependent roughness that may alter wetting stability under real environmental stressors. Therefore, a central challenge is identifying how AM processing parameters, surface designs and environmental influences collectively govern wetting durability and corrosion resistance, particularly when applied to industrially relevant metallic systems.

This review addresses interconnected challenges by examining corrosion control strategies through the lens of additive manufacturing. It evaluates environmental influences governing corrosion initiation and progression, outlines main mechanisms and limitations of superhydrophobic anticorrosion surfaces and discusses how AM-based processing can enable geometry-specific and functionally engineered protective layers. By integrating insights from corrosion science, surface engineering and additive manufacturing, this review aims to provide a structured understanding of how superhydrophobic design and AM processing can be aligned to support next-generation corrosion management for pipelines and related infrastructure exposed to harsh service environments.

1.1 CORROSION MECHANISMS IN SOIL

Corrosion is an electrochemical process that occurs when a metal interacts with its environment. It involves two primary reactions, oxidation and reduction, which take place at different locations on the metal surface, creating an electrochemical cell. Formation of rust (Fe_2O_3) in ferrite compounds can be represented by the following chemical reactions involving iron (Fe), hydroxyl ion (OH^-), oxygen (O_2) and water (H_2O)

$$Fe^{2+} + 2OH^- \rightarrow Fe(OH)_2 \quad (3)$$

$$4Fe(OH)_2 + O_2 + 2H_2O \rightarrow 4Fe(OH)_3 \quad (4)$$

$$2Fe(OH)_3 \rightarrow Fe_2O_3 + 3H_2O \quad (5)$$

Scheme 1 represents the origins of corrosion occurring via different mechanisms. These mechanisms are well understood and studied, resulting in various solutions for corrosion prevention and reduction.

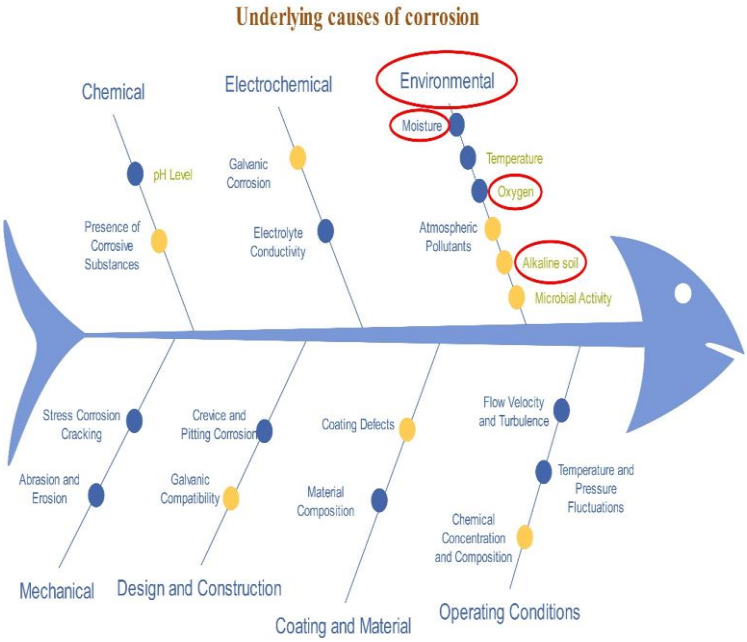

Scheme 1. Fishbone diagram for corrosion origins

The chemical composition of the soil is predominantly determined by the compounds present in the water, which may exhibit either a basic nature, exemplified by sodium, potassium, calcium and magnesium, or an acidic disposition, as exemplified by chlorides, sulphates and carbonates]. Soluble nature of salts, as well as concentration, along with moisture content, primarily dictate the soil's capacity to conduct electric current, a main factor in the context of corrosion processes.

Steel corrosion in alkaline soil

In alkaline soil, steel is prone to both uniform corrosion (rust) and localized pitting, with the specific mechanism being highly dependent on the concentration of various ions in the soil. The primary electrochemical reactions involve the reduction of oxygen at the cathode and the dissolution of iron at the anode. The process is heavily influenced by moisture, which facilitates ion transport, and the presence of aggressive ions like chlorides, sulfates and bicarbonates. Gadala et al. determined that in aerated, alkaline soil solution the following processes on X70 steel occur:

- The cathodic reaction is dominated by the reduction of oxygen:

$$3/2\,O_2 + 3H_2O + 6e \rightarrow 6OH^- \quad (6)$$

This is generally considered as the dominant corrosion mechanism in alkaline soil, occurring in the presence of water in soil.

- The anodic process involves the dissolution of steel and the formation of different iron compounds:

$$Fe \rightarrow Fe^{2+} + 2e \quad (7)$$

$$Fe^{2+} + 2OH^- \rightarrow Fe(OH)_2 \rightarrow FeO + H_2O \quad (8)$$

$$4Fe(OH)_2 + O_2 + 2H_2O \rightarrow 4Fe(OH)_3 \quad (9)$$

$$4Fe(OH)_2 + O_2 \rightarrow 2Fe_2O_3 + 4H_2O \quad (10)$$

$$Fe(OH)_3 \rightarrow FeOOH + H_2O \quad (11)$$

[36] [37] [38]. Soil can contain various aggressive ions, such as chlorides or sulphates, which can exacerbate the corrosion of steel. The important factors that influence corrosion are:

- Presence of bicarbonates and carbonates

Bicarbonate (HCO_3^-) is particularly significant in the dissolution of pipeline steels, contributing to the formation of iron carbonate ($FeCO_3$) [39]. The associated chemical reactions are:

$$2H_2CO_3 + 2e^- \rightarrow H_2 + 2HCO_3^- \quad (12)$$

$$2HCO_3^- + 2e^- \rightarrow H_2 + CO_3^{2-} \quad (13)$$

- Presence of chlorides

In the presence of chloride ions, dissolved iron from the anodic process attracts negative Cl^- ions, which hydrolyze to form hydrochloric acid (HCl), increasing local acidity and promoting pitting corrosion through an autocatalytic mechanism [40].

$$FeCl_2 + 2H_2O \rightarrow Fe(OH)_2 + 2HCl$$

- High-pH environment

High pH (9-11) can induce intergranular SCC, a dangerous form of damage where cracks form and propagate along the grain boundaries of metal. Stress corrosion cracking (SCC) can be defined as the interaction of tensile stress with a corrosion environment on a susceptible metallic surface resulting in the initiation and propagation of cracks].

- Material composition and microstructure

Next to the soil composition, the corrosion behavior of steel is also affected by its microstructure. Heat treatments that result in bainite and martensite phases increase the steel's electrochemical activity. The presence of pearlite can enhance the corrosion rate of ferrite due to galvanic effects [46]. Different steel grades exhibit varying corrosion resistance; for instance, in saline soil, after 360 days of exposure, the general order of corrosion rates was found to be Q235 > X65 ≈ X70 > X80 (Figure 2) [*Sebastian et al., 2018*].

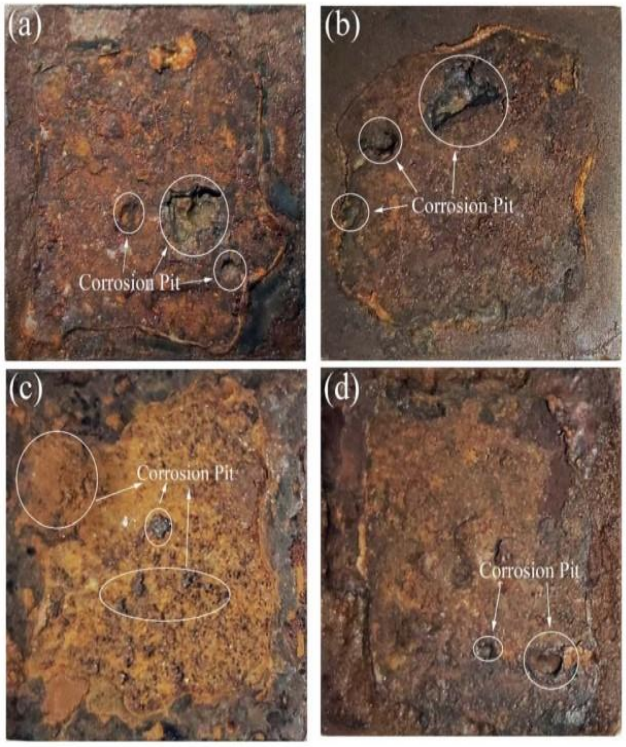

Figure 2. Macroscopic corrosion of steel after 360 days: a) q235, b) X65, c) X70, d) X80 [33]

Numerous researchers have conducted electrochemical investigations employing soils as surrogates for real-world service conditions, in order to enable future service-time prediction and protection methods for steel pipes. Liu et al. conducted electrochemical tests to scrutinize the influence of electrolyte composition. Potentiodynamic tests revealed that the additional cations exhibited aggressiveness in

the following order: $K^+ > Mg^+ > Ca^{2+}$, while the anions' aggressiveness ranked as $SO_4^{2-} > HCO_3^- > NO_3^-$. Noor et al. conducted research from different soils, depending on pH [50]. They concluded that alkaline soil was less corrosive compared to acid environment. Similar conclusion was reported by Benmoussa et al., which utilized electrochemical tests to explore the factors influencing the aggressiveness of a solution designed to emulate a basic soil (comprising KCl, $NaHCO_3$, $CaCl_2$, and $MgSO_4$) from Algeria [51]. They discovered that the solution's aggressiveness heightened with increased acidity and temperature. Based on the knowledge on corrosion origins, different protection techniques have been proposed.

2.2 Corrosion in Acidic Soils

Steel corrosion in acidic environments is a major concern, particularly in the presence of strong acids and chlorides, where it is highly susceptible to pitting [52,53]. The corrosion process in acidic media is driven by the reduction of hydrogen ions at the cathode and the oxidation of iron at the anode.

- **Anodic Reaction:** $Fe \rightarrow Fe^{2+} + 2e^-$
- **Cathodic Reaction:** $2H^+ + 2e^- \rightarrow H_2$
- **Overall Reaction:** $Fe + 2H^+ \rightarrow Fe^{2+} + H_2$

The acceleration of metal corrosion rates is facilitated by the dissociation of potent acids such as HCl, HNO_3, and H_2SO_4 in the galvanic cell. In the presence nitric acid, a strong oxidizing agent, the anion assumes a significant role in the oxidation process compared to the cation, steel undergoes a reaction, resulting in the formation of an oxide layer, iron(II) nitrate on the metal surface. Initially serving as a protective barrier, oxide layer prevents direct contact between the metal and the acid, inhibiting further reaction. However, this brittle oxide layer experiences repeated exfoliation, leading to the reestablishment of metal-acid contact and causing severe dissolution of the metal surface, resulting in significant corrosion. When exposed to non-oxidizing acids like HCl, steel reacts to produce iron salts (II) (e.g., $FeCl_2$) as a corrosion product. Hydrochloric acid induces rusting in carbon steel through a process known as autocatalytic corrosion. Similarly, contact with H_2SO_4 leads to the formation of $FeSO_4$. The corrosion of the metals is highly influenced by the concentration of the corrosive agent and the duration of exposure. With increased concentration and exposure time, the rate of metal dissolution rises. In order to slow corrosion and increase service time, coatings and inhibitors are usually employed.

CONVENTIONAL PROTECTION STRATEGIES

While some protection methods are tailored to a specific pH range, modern approaches have evolved from simple passive barriers to active, multifunctional systems designed to be versatile and effective across both acidic and alkaline conditions. Numerous studies have focused on the application of advanced coatings and inhibitors for robust steel protection, though many have focused on near-neutral pH environments [*Sebastian et al., 2018*]. This section reviews several classes of advanced coatings and smart inhibitor systems that represent the frontier of corrosion science.

3.1 Galvanization and cathodic protection

Cathodic protection is widely applied as an active corrosion control strategy for steel pipelines, particularly in buried or submerged environments where electrolyte contact is unavoidable. In practice, cathodic protection systems are commonly implemented through sacrificial anodes (galvanic protection) or impressed current cathodic protection (ICCP), both of which operate by shifting the steel surface potential into a range where anodic dissolution is suppressed. Sacrificial anodes such as magnesium (Mg) and zinc (Zn) are frequently selected due to their sufficiently negative electrode potentials, enabling them to preferentially corrode and supply protective current to the steel structure. This approach has been shown to significantly reduce steel corrosion rates even under challenging conditions such as alternating current (AC) interference, which may occur near electrified railways or high-voltage power lines. Under such circumstances, cathodic protection can maintain substantial protective performance, with reported protection efficiencies exceeding 76%, thereby mitigating the risk of AC-induced corrosion and limiting localized damage development. Nevertheless, system effectiveness remains dependent on soil

resistivity, coating condition, electrical continuity and current distribution, meaning that inadequate design or shielding effects may lead to under-protected regions and persistent corrosion activity.

Galvanization represents another established corrosion protection route, where steel is coated with a zinc layer that provides both barrier protection and sacrificial behavior. In alkaline environments, galvanized steel may develop compact and adherent oxide or hydroxide-based surface layers that slow down further corrosion by restricting ionic transport and reducing metal dissolution rates]. However, this passivation behavior is highly sensitive to environmental chemistry. In the presence of sulfate-containing media, passivation may be disrupted, as sulfates can promote the formation and precipitation of coarse calcium hydroxy zincate phases [66]. These deposits are often less protective, can impair layer uniformity, and may accelerate localized corrosion processes, ultimately leading to severe deterioration despite the initial protective intent of the zinc coating.

3.2 Protective coatings

Modern protective coatings aim to provide not just a simple physical barrier but also functionalities like self-healing, stimuli-responsive protection, and enhanced durability through structural and chemical modification [67,68].

Organic-based coatings represent a dominant strategy for enhancing the barrier properties, mostly relying on the incorporation of nanofillers into a polymer matrix]. Fillers, such as nanoclays, graphene or carbon nanotubes, create a highly tortuous pathway for corrosive media. This structure significantly slows the diffusion of aggressive species like water, oxygen, and chloride ions to the metal substrate, thereby enhancing the coating's protective lifetime. A wide range of nanofillers have been investigated; for instance, incorporating 2D materials like MXene ($Ti_3C_2T_x$) into silicate-bonded ceramic coatings has shown superior anti-corrosion performance in H_2SO_4, NaOH and NaCl solutions. Hexagonal boron nitride (h-BN) nanosheets combined with polyaniline incorporated in epoxy have also been shown to significantly enhance the protection of mild steel in saline environment. Bio-based resins derived from sources like cardanol are being developed to create more sustainable and durable coatings, including polyurea-epoxy composites with antibacterial properties and polyurethane nanomaterials with embedded nano-silver. Mussel-inspired chemistries using biomass-modified graphene are also being explored for fully bio-based epoxy systems with strong adhesion and corrosion resistance. Recently, highly functional macromolecules, such as phosphorus-based dendrimeric resins, opened another route to creating highly durable and effective anticorrosive coatings. Another important class in corrosion protection are superhydrophobic coatings, inspired by natural surfaces, like the lotus leaf, creating a water-repellent surface with a water contact angle greater than 150°]. This property establishes a stable air layer (plastron) between the coating and the environment, which acts as a physical barrier preventing the corrosive electrolyte from contacting the surface.

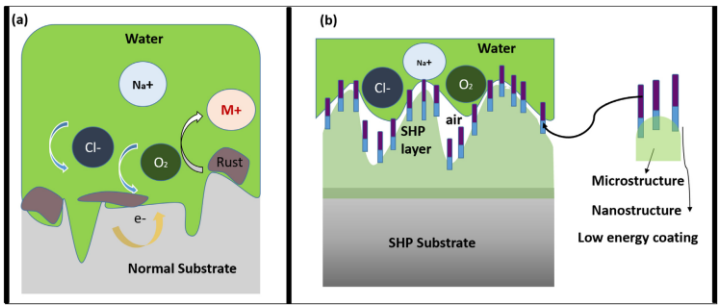

Figure 3. An illustration of a coated and uncoated substrate placed within a corrosive environment, showing: (a) the development of an electrolyte film on the substrate that is uncoated, and (b) how a plastron layer prevents direct interaction between the corrosive medium and the substrate when a superhydrophobic surface is submerged in a corrosive electrolyte [60].

Superhydrophobic coatings can be effective in both acidic and alkaline environments. For example, an electrodeposited

superhydrophobic conducting polythiophene coating demonstrated exceptional corrosion protection (efficiency > 95%) for steel substrates immersed in chloride solutions of varying pH]. More recently, simple spray-on methods have been used to create ETFE-ZrO_2 composite coatings with contact angles over 157° and corrosion current densities an order of magnitude lower than bare steel, maintaining excellent chemical stability across a wide pH range (3 to 12). The more thorough review on superhydrophobic surfaces is presented in separate subsection 3.1.

Inorganic-based coatings are durable and sustainable alternatives to polymers, which have gained attention parallel with organic-based solutions [80]. This category includes sol-gel coatings, which can be applied in single or multi-layer systems to create dense, protective films. Other advanced inorganic coatings include Cr_2AlC MAX phase materials, which exhibit superior corrosion resistance when deposited on stainless steel [81]. Geopolymer coatings, which form a dense, three-dimensional aluminosilicate network, can effectively impede chloride migration [82]. Modifications with polyvinyl alcohol (PVA) and nano-TiO_2 create a highly effective coating that forms strong Si-O-Fe chemical bonds with the steel surface. Another promising and environmentally favorable option is magnesium phosphate cement (MPC) coating, which provides protection through both a physical barrier and chemical passivation from excess MgO in the mix [*Sebastian et al., 2018*].

3.3 Smart self-healing and inhibitor release systems

A significant progress in corrosion protection involves the development of smart coatings that can autonomously respond to local damage. This is most often achieved by encapsulating corrosion inhibitors in micro- or nanocontainers that are dispersed throughout the coating matrix, which enables overcoming the major limitations of directly adding inhibitors that can compromise the coating's mechanical properties, interfere with the curing process and leach out prematurely [84]. The nanocontainers are engineered to release their inhibitive payload in response to a local corrosion trigger, such as a change in pH at the coating-metal interface [85]. A variety of materials are used for nanocontainers, including mesoporous silica, layered double hydroxides, and zeolitic imidazolate frameworks (ZIF-8), which can be loaded with *green* inhibitors like 8-hydroxyquinoline (8HQ) or bio-polymers such as chitosan and its derivatives.

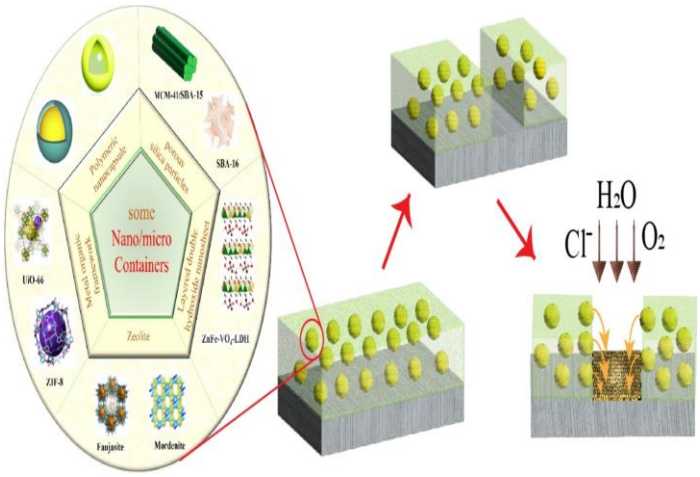

Figure 4. Illustration of the release of inhibitors by nano/microcontainers to passivate the substrate in a defect region .

Furthermore, the development of green inhibitors from plant extracts, such as *Gliricidia sepium*, combined with silica hybrids, represents a sustainable approach to creating effective anticorrosive systems. Similarly, bio-nanocomposites of phytochemicals like bergenin and malabaricone C encapsulated in mesoporous silica have been successfully integrated into smart epoxy coatings.

3.4 Limitations of conventional corrosion protection

While conventional methods such as coatings, cathodic protection, inhibitors and material selection are the cornerstones of corrosion management, they possess inherent limitations that prevent the complete elimination of degradation. Table 1 summarizes the advantages and disadvantages of corrosion protection methods discussed in this review.

⇒ **Cathodic protection (CP) -** Protection based on CP requires regular monitoring and maintenance to ensure the anodes and power systems are functioning correctly, which can be

costly and logistically challenging for extensive pipeline networks]. A primary technical challenge is shielding, where the protective electrical current is blocked from reaching parts of the steel surface by disbonded coatings, complex geometries or external barriers]. Additionally, excessive current (over-protection) can cause hydrogen embrittlement in high-strength steels and accelerate coating disbondment.

⇒ **Protective coatings -** Organic polymer coatings are prone to weathering and degradation from environmental stressors like UV radiation, ozone and thermal shock [92–94]. Furthermore, micropores, cracks and other defects can form during application and curing, creating diffusion pathways for corrosive species like water, oxygen and chlorides [95]. Once a coating is breached, it can create an unfavorable anode-to-cathode area ratio, leading to localized pitting that can penetrate a pipe wall much faster than uniform corrosion. The issue is compounded by challenges in achieving optimal compatibility between fillers and the polymer matrix, which can lead to aggregation and compromise barrier properties, or by poor coating adhesion, a phenomenon known as cathodic disbondment or delamination. Even endurable epoxy-ceramic coatings can fail due to microbially influenced corrosion (MIC), where biofilms create aggressive microenvironments that lead to blistering and crevice corrosion.

⇒ **Corrosion inhibitors -** Chemical inhibitors must be continuously replenished to remain effective, and their performance is highly dependent on environmental conditions such as temperature, pH and flow rate *Sebastian et al., 2018*. Many traditional inhibitors, like chromates, are now restricted due to their toxicity and environmental impact. While *green* inhibitors derived from natural sources are gaining popularity, they often exhibit lower inhibition efficiency, and developing highly effective, environmentally friendly options remains an active area of research. Furthermore, the direct addition of inhibitors into a coating matrix can disrupt the curing process, interfere with adhesion, and compromise the coating's mechanical properties *(Sebastian et al., 2018*.

⇒ **Material selection -** The most significant limitation of using high-performance corrosion-resistant alloys (CRAs) like stainless steel is their high initial cost compared to carbon steel [89]. These materials can also present fabrication challenges (e.g., welding) that require specialized techniques and quality control. Moreover, CRAs are not immune to corrosion; they can suffer from severe localized corrosion, such as pitting, crevice corrosion and stress corrosion cracking (SCC), in specific aggressive environments like those containing high chloride concentrations or elevated temperatures. The choice of material is also limited by availability and compatibility with other manufacturing processes.

Table 1. Advantages and disadvantages of different conventional anticorrosive protections for steel

Protection method	Advantages	Disadvantages	Study
Cathodic protection (CP)	• Very effective for large structures, protects coating defects • Adjustable and controllable	• Requires constant monitoring and maintenance • Risk of hydrogen embrittlement and shielding effects	[89–91]
Galvanization	• Provides both barrier and sacrificial protection • Cost-effective for many applications	• pH-sensitive and has a finite lifespan • Vulnerable to certain ions	[64–66]
Polymer nanocomposite coatings	• Superior barrier properties, mechanical strength and adhesion • Highly versatile and adaptable with various nanofillers	• Risk of nanofiller agglomeration creating defects • Higher cost and potential compatibility issues	[69–74]
Superhydrophobic coatings	• Creates a stable air barrier to prevent electrolyte contact • Self-cleaning and effective across a wide pH range	• Mechanically fragile and susceptible to abrasion • Poor long-term stability and complex fabrication	[78,79]

Inorganic-based coatings	• Highly durable, thermally stable and eco-friendly • Forms strong chemical bonds with the steel substrate	• Brittle and prone to cracking under mechanical stress • Complex application and can be porous before full cure	[80–83]
Self-healing coatings	• Autonomous, on-demand inhibitor release repairs micro-damage • Extends coating lifetime and improves long-term efficiency	• Limited inhibitor payload and finite healing capacity • Increased complexity and cost of formulation	[84–88]
Corrosion inhibitors	• Cost-effective and easy to apply in closed systems • Can be highly efficient for specific environments	• Often require continuous replenishment • Many are toxic; can degrade coating properties if added directly	[97–102]

1 3D PRINTING FOR CORROSION PROTECTION

3D printing, or additive manufacturing (AM), is a process of creating three-dimensional objects by adding material layer by layer [106]. AM technologies enable the production of a wide range of prototypes or functional components with complex geometries that are difficult or impossible to manufacture using conventional methods [107,108]. Compared to traditional methods, AM can shorten the design-to-manufacturing cycle, reduce production costs, and enhance competitiveness]. Furthermore, with advancements in processes and modelling/design [*Sebastian et al., 2018*], AM technologies have seen broader application over the past three decades. 3D printing has the potential to revolutionize corrosion protection methods by enabling innovative approaches to surface modification, material selection, and design optimization. Superhydrophobic surfaces can be obtained by the geometry control of the coating. There are several 3D printing techniques available, each with its own advantages and disadvantages. Figure 5 illustrates different 3D printing techniques [*Huang et al., 2026)*].

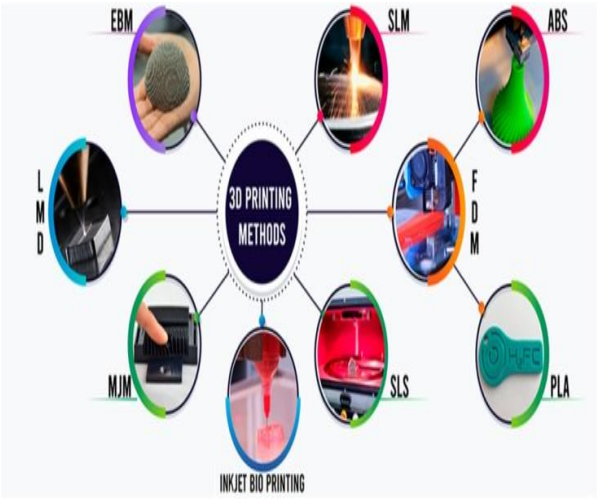

Figure 5. Classification of 3D printing techniques [43]

In the following subsections, FDM technique will be described, including its application for anticorrosive coatings processing.

4.1 Fused Deposition Modelling (FDM)

Fused Deposition Modeling (FDM) is a prevalent and cost-effective additive manufacturing (AM) technique that fabricates three-dimensional components by extruding a molten thermoplastic filament layer-by-layer [116]. Its widespread use is due to its simplicity and compatibility with a broad range of polymers, such as PLA and ABS *Adabavazeh et al., 2024*]. The process starts with a digital 3D model that is sliced into horizontal layers. During printing, the filament is melted in a heated extruder and precisely deposited onto a build platform. Each layer cools and solidifies, bonding to the previous one until the object is fully formed. The operational principle of an FDM system is shown in Figure 6, and its advantages and limitations are outlined in Table 2.

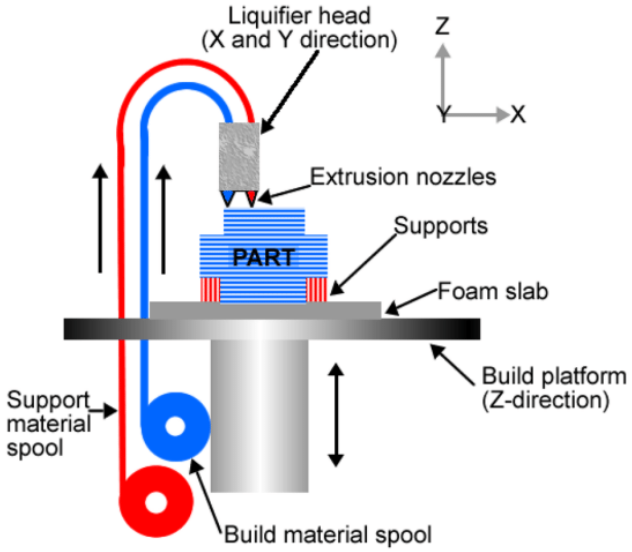

Figure 6. Scheme of FDM working principle

Table 2. Advantages and disadvantages of FDM

3D printing technique	Advantages	Disadvantages
FDM	• Affordability • Material Variety • Large Build Volume • Ease of Use • Support Structures	• Layer Resolution • Surface Quality • Limited Material Strength

With a wide range of materials (Figure 7) and possibility to form layer-by-layer re-entrant geometry that results in repellent surface even in materials that are not hydrophobic in nature, FDM stands out as a potential technique for anticorrosive protection surfaces.

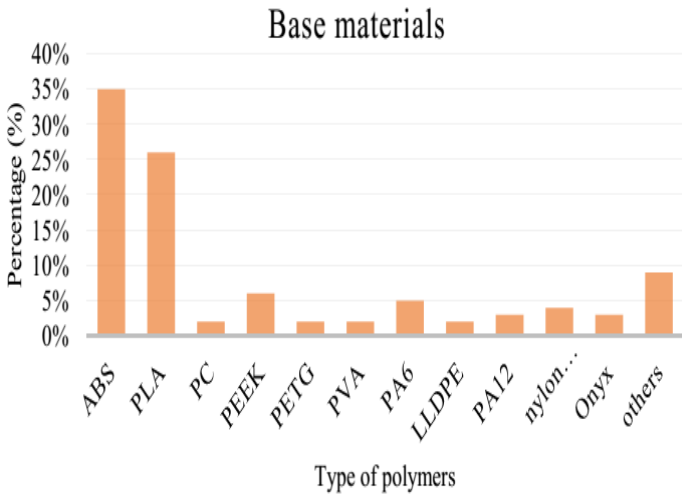

Figure 7. Commonly used materials for FDM 3D printing [120]

Furthermore, unlike techniques using liquid materials, FDM offers the possibility of direct deposition of filament on the pipe surface, without additional cleaning and waste generation. However, limited level of details, required post-processing and possible layer de-bonding represent challenges and limitation in the application of this technique. FDM finds applications in various industries, from drug delivery in medicine to aerospace applications].

4.2 Potential application of 3d printing for corrosion protection

3D printing presents unique method for corrosion protection, which could enable surface modification techniques, material selection, and design optimization strategies, 3D printing enables the creation of corrosion-resistant components and structures. It can be utilized to deposit corrosion-resistant coatings directly onto the metal surface. This enables precise control over coating thickness and composition, enhancing protection against corrosive environments. By incorporating additives and nanomaterials into the printing process, surfaces can be functionalized with properties like self-healing, anti-fouling or improved resistance to specific corrosive agents. Materials with low surface energy are repellent to water, with high contact angles, which is an important anticorrosive feature. Advanced corrosion-resistant materials, such as high-performance polymers, stainless steels, titanium alloys can be used for printing of functional surface. 3D printing enables the integration of reinforcing materials, such as fibres or nanoparticles, into polymer matrix to create composite structures with improved corrosion resistance. Furthermore, design of complex geometries and customized designs that minimize crevices, sharp edges and other corrosion-prone areas is enabled. Topology optimization techniques can be applied in 3D printing to optimize the design of structures for enhanced corrosion resistance. By distributing material efficiently, stress concentrations and potential corrosion sites can be minimized. Computational modelling and simulation tools can be utilized in conjunction with 3D printing to predict corrosion behaviour, optimize designs and assess the effectiveness of corrosion protection strategies.

4.3 Processing of hydrophobic and superhydrophobic coatings by using FDM

In superhydrophobic surfaces, typically defined by a CA above 150°, air pockets become trapped within the micro- or nanostructured features (Cassie-Baxter state), which minimizes the actual contact area between the liquid and the substrate. Figure 8 shows the difference between hydrophilic, hydrophobic and superhydrophobic surface in contact with water droplet.

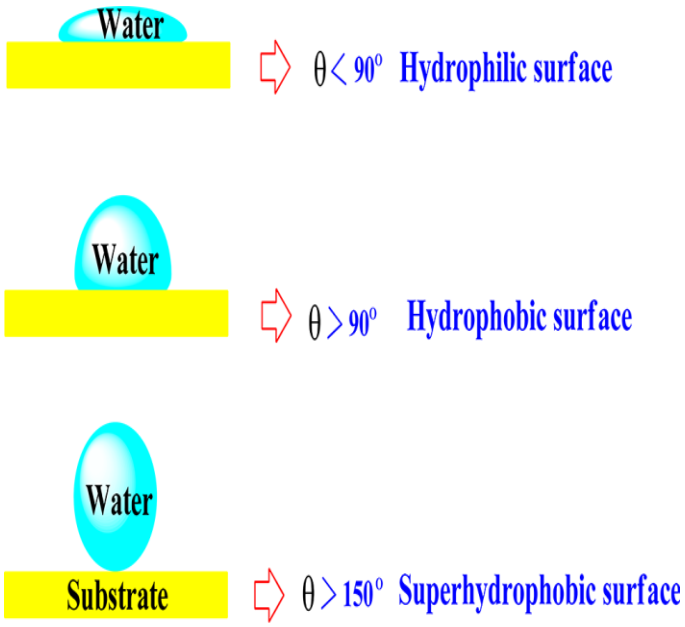

Figure 8. Schematic illustrations of hydrophilic, hydrophobic and superhydrophobic surfaces [133]

The reduction in contact area limits the adsorption of water and corrosive species, such as chloride ions, thereby inhibiting the electrochemical reactions that drive corrosion processes. Studies have shown that as the CA increases, the corrosion current density measured by potentiodynamic polarization techniques decreases significantly, and the charge transfer resistance determined by electrochemical impedance spectroscopy (EIS) increases. Several studies have reported high contact angles achieved by using 3D printing techniques for the processing of superhydrophobic coating. Material extrusion methods, particularly FDM, are the most widely used for fabricating superhydrophobic surfaces due to their low cost and versatility. Several strategies have been employed using this technique.

4.3.1 Direct printing and post-processing

Another common strategy is to directly print a part and then modify its surface through physical or chemical treatments.

Using inherent roughness directly – The surface roughness from the FDM process itself can be harnessed without post-processing. Kingman and Dymond found that by varying printing parameters, such as increasing layer height and raster width on PLA parts, this anisotropy could be enhanced, leading to partial wetting and contact angles exceeding 120° perpendicular to the tool path. Atwah et al explored the direct fabrication of water-repellent, self-cleaning 3D-printed textile-like structures investigating different polymers [].Three flexible thermoplastic filaments were selected as feedstock materials: thermoplastic polyurethane, thermoplastic elastomer and thermoplastic co-polyester, achieving the highest WCA for thermoplastic elastomer (149°), with the investigation of differences between materials and printing parameters.

Post-processing – A printed structure can be modified with subsequent treatments to add superhydrophobic properties. A common approach involves dip-coating a printed part in a solution containing nanoparticles. Lee et al. printed PLA samples and then dip-coated them in a solution of hydrophobic fumed silica nanoparticles, which adhered to the partially dissolved surface to create a hierarchical nano/microscale structure with a WCA greater than 150°. In a similar manner, Zhao et al. created shape-memory microplate arrays and then applied a sprayed coating of a PDMS/SiO_2 solution to achieve reversible super hydrophobicity. Taking post-processing a step further, Zhan et al. combined FDM 3D printing of a PLA micropillar array with magnetron sputtering to deposit a copper film, followed by chemical modification with a stearic acid ethanol solution to create a dual-responsive (optically and thermally) shape-memory surface Amin et al. fabricated PLA surfaces with pyramidal microstructures and used chemical etching in hydrogen fluoride (HF) to enhance the roughness before applying a low surface energy coating. A different approach was taken by Bai et al., who 3D printed a bio-inspired cellular origami structure and then applied a chemical treatment to render it superhydrophobic. This design, inspired by water striders and diving bell spiders, uses trapped air in its cells to achieve remarkable floatability and resistance to sinking. The principle of their innovative design is presented in Figure 9.

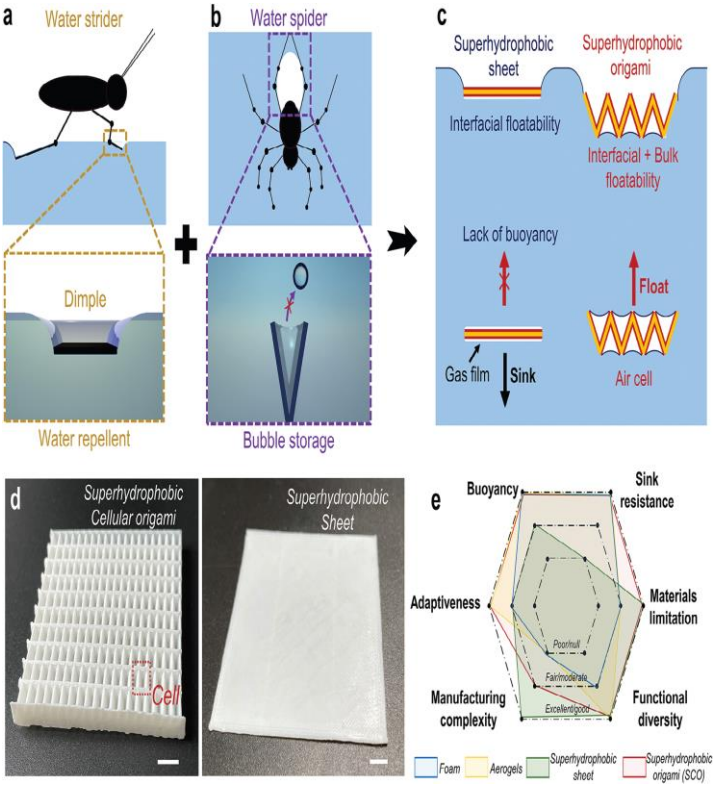

Figure 9. The design principle of the multi-bioinspired superhydrophobic cellular origami (SCO). A) Superhydrophobic surface inspired by water strider b) Superhydrophobic air cell inspired by the diving bell spider, which could store air underwater and provide abundant buoyance. C) The designed bionic SCO integrates the superhydrophobic surface and the air cell, which is capable of sink resistance. D) Optical image of the superhydrophobic cellular origami and the superhydrophobic sheet. Scale bar is 5 mm. e) Comparison of floating properties of SCO and other materials, including foam, aerogels, superhydrophobic sheet and SCO..

Design of re-entrant surface geometry reduces penetration of water into the surface by air entrapment. Figure 10 shows the amphiophobic surface prepared by Shams et al., using FDM for printing re-entrant geometry and surface treatment for porosity; they determined that the printing direction was crucial for achieved contact angles [*Yu et al., 2025*].

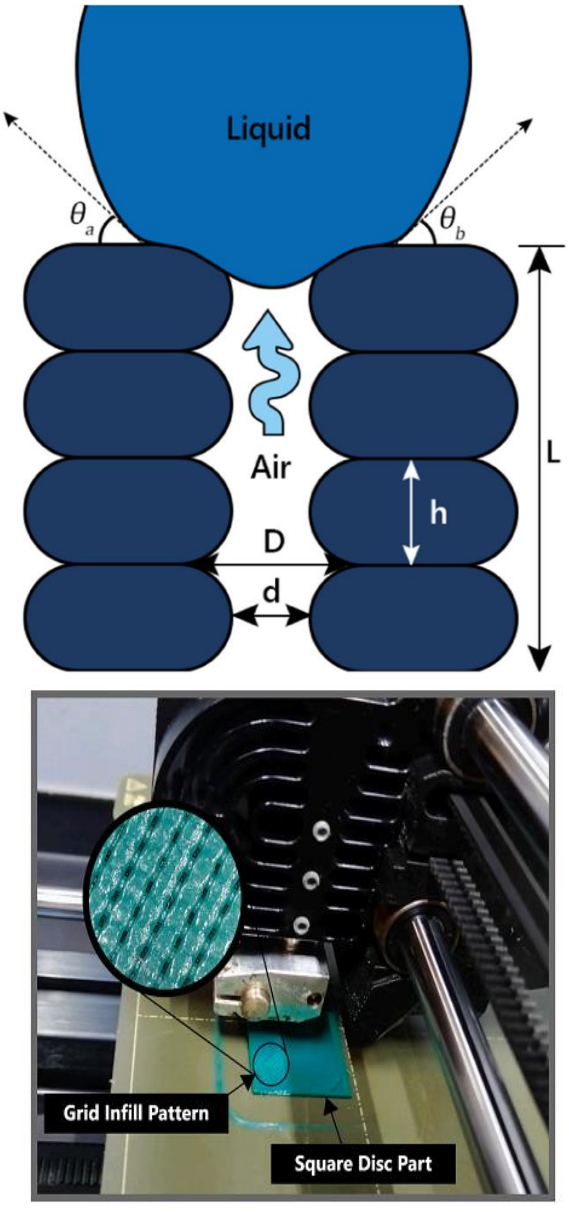

Figure 10. a) Illustration of air entrapment between two printed structures (θ_a is left contact angle, θ_b is right contact angle, D is groove spacing between two adjacent inside edges, d is groove spacing between two adjacent outside edges, h is the layer height and L is the length of overall printed structure); b) 3D printing of amphiophobic disc specimens [*Huang et al., 2026)*]

4.3.2 Indirect fabrication via 3D printed molds

A highly effective method involves using FDM to print molds from which the final surfaces are cast, which is why it is called indirect. This strategy preserves the geometric freedom of additive manufacturing while enabling the fabrication of fine and highly controlled microstructures through replication, avoiding the resolution limitations and stair-stepping artifacts commonly associated with direct printing using low-cost FDM. Recently, indirect replication has been recognized as a practical route for producing liquid-repellent and self-cleaning surfaces, as it enables scalable microstructure generation while allowing the final functional surface to be manufactured from elastomers or composite materials that may not be easily processed by standard FDM printing [*Huang et al., 2026)*]. In the context of functional anti-wetting structures, indirect strategies are also discussed as promising solutions to overcome limitations in durability and structural fidelity encountered in several direct-printing approaches.

Exploiting inherent mold roughness - The natural surface texture of FDM prints can be transferred to a cast material. Kang and colleagues demonstrated this by printing polylactic acid (PLA) molds with pyramidal structures, finding that lower printing resolutions produced rougher molds [144]. When polydimethylsiloxane (PDMS) was cast from molds, the transferred roughness made the resulting PDMS surfaces highly hydrophobic, achieving a water contact angle (WCA) of approximately 143°. In a follow-up study, they varied the printing angle of the mold from 0° to 90°, creating cast PDMS surfaces with tilted, waveform microstructures that achieved superhydrophobicity with a WCA of 160° and a roll-off angle of just 8° [145]. This process-structure linkage is consistent with broader wetting theory, where achieving high WCA together with low roll-off/low hysteresis is associated with stable Cassie-Baxter wetting states supported by air entrapment within surface asperities [146].

Specific structures - The mold can be designed to create highly specific and functional topographies. Duran et al. utilized FDM to create molds where the sharp, acute angle formed between rounded printed filaments could be exploited [*Yu et al., 2025*]. When replicated with PDMS, this feature formed reentrant structures capable of repelling both water (WCA of 160°)

and low-surface-tension liquids like ethylene glycol, demonstrating amphiphobicity. Illustration of indirect processing via FDM is presented in Figure 11. This approach offers a low-cost route to amphiphobic re-entrant structures through where edge-angle control is critical for liquid repellence, feature difficult to produce directly via common AM routes.

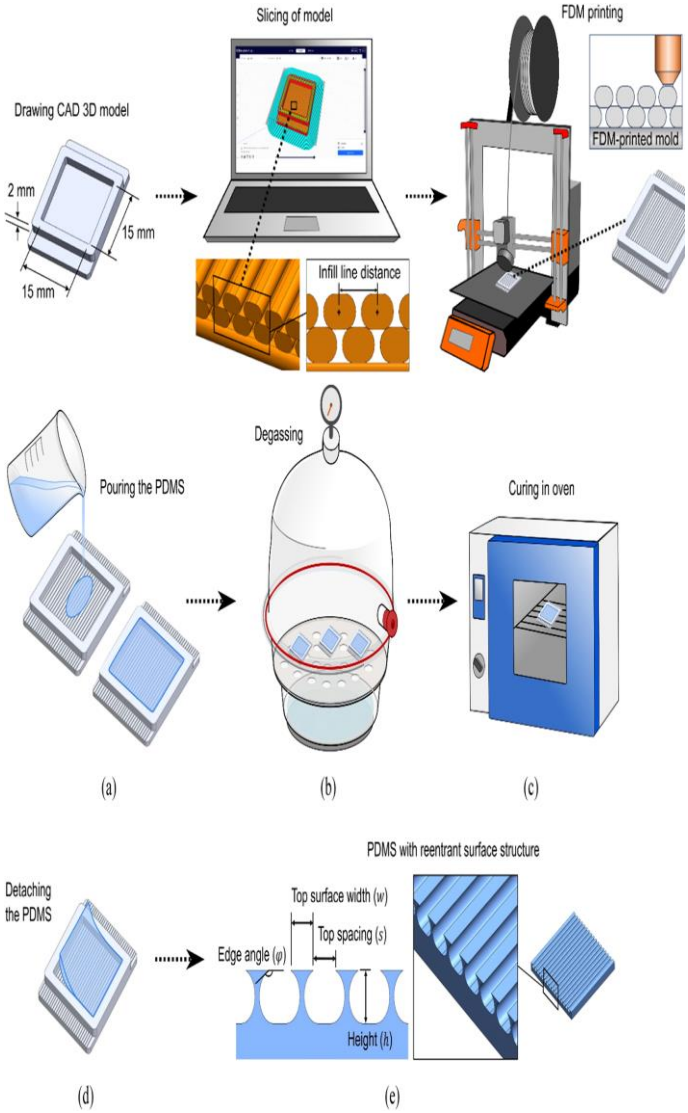

Figure 11. Schematic illustration of mold processing by FDM and preparation of PDMS superhydrophobic sample

Manderfeld et al. also used FDM-printed molds to cast a conductive graphite-carbon black-silicone composite [148]. The resulting microstructured surfaces, with a WCA over 150°, could form a stable underwater air layer (plastron) that inhibits biofouling and can be replenished through Joule heating.

Table 3. Summary of achieved WCA using FDM

Study	Printing Techni	Material (s)	Fabrication Strategy	Achieved WCA
Bai et al. [124]	FDM (Direct)	Polymer, R972 particles	Printed an origami structure followed by chemical corrosion and particle coating.	~146°
Lee et al. [121]	FDM (Direct)	PLA, Silica NPs	Dip-coating of a printed part with silica nanoparticles.	>150°
Zhao et al. [121]	FDM (Direct)	PLA, PDMS/SiO_2	Spraying with PDMS/SiO_2 solution.	160°
Zhan et al. [122]	FDM (Direct)	PLA, Copper	Magnetron sputtering + chemical modification.	166.3°
Amin et al. [141]	FDM (Direct)	PLA	Printed pyramids + chemical etching.	142.0°
Atwah et al. [137]	FDM (Direct)	TPE, TPU, TPC	Optimized layer height, extruder width, and orientation for self-cleaning fabrics.	149°
Barrios & Romero [149]	FDM (Direct)	PETG	Optimized printing parameters (acceleration, flow rate) for self-cleaning.	~108°
Wang et al. [129]	FDM (Direct)	PLA, Mullite	Developed a composite filament with mullite filler for bulk hydrophobicity.	>150°
Shams	FDM	PLA	Optimized	~120°

et al. [105]	(direct)		surface treatment and printing parameters for self-cleaning.	
Duran et al. [127]	FDM (Indirect)	PLA, PDMS	Cast PDMS from a mold designed with sharp angles to form reentrant structures.	160°
Manderfeld et al. [148]	FDM (Indirect)	PLA, Silicone Composite	Cast a conductive silicone composite from a micro-structured mold.	>150°
Kang et al. [125]	FDM (Indirect)	PLA, PDMS	Cast PDMS from a mold printed at various angles to create waveform structures.	160°
Kang et al. [126]	FDM (Indirect)	PLA, PDMS	Cast PDMS from a low-resolution printed mold with pyramidal structures.	~143°

As can be observed, simple technique like FDM could be used for obtaining high contact angles, which is the most important step in reducing the impact of harmful environment on steel.

4.4 Influence of 3D printing parameters on contact angle

For achieving high water contact angles and stable water-repellent behavior, it is essential to understand how 3D printing parameters govern surface morphology, topology and anisotropy, as well as how these surface properties control droplet wetting, pinning and mobility. In extrusion-based additive manufacturing, particularly fused deposition modelling (FDM), the surface is not an idealized, smooth interface, but a hierarchical structure composed of filament ridges, inter-road valleys, stair-stepping features and interlayer seams [*Oni et al., 2025*]. Consequently, the apparent water contact angle (WCA) measured on 3D-printed parts is determined by a complex interplay between intrinsic polymer surface energy and the printing-induced micro- and meso-scale architecture [*Oni et al., 2025*].

- Influence of layer orientation and height

A foundational contribution to the understanding of parameters' influence on materials hydrophobic properties gave the work of **Kingman and Dymond**, who systematically demonstrated that wettability on FDM-printed PLA is **anisotropic and parameter-dependent**, rather than an intrinsic material constant [136]. By separating intrinsic contact angle (measured on smooth extrudate) from apparent contact angle (measured on printed surfaces), they showed that the printed texture alone is sufficient to induce substantial changes in WCA. The authors reported that when water contact angle is measured on surfaces perpendicular to the build direction, increasing layer height led to an increase in the average WCA. Their contact angles increased from approximately 92.8 ± 8.8° at a layer height of 0.05 mm to 108.5 ± 4.0° at a layer height of 0.25 mm *Adabavazeh et al., 2024*. This outcome highlights that larger layer heights can generate anisotropic ridges and topographical barriers that hinder droplet spreading and can increase hydrophobic response under certain measurement orientations. In the study of Neukäufer et al. layer orientation has proved to be an important contributor for the CA in printed polypropylene samples. In randomly packed samples, CA was below 90°, while in 90° orientation, it reached around 123°. This transition from non-hydrophobic to clearly hydrophobic behavior, achieved without altering material chemistry, highlights the role of layer arrangement in controlling surface texture continuity and droplet-surface interaction. Sung et al. demonstrated the influence of layer height by introducing a layer height modulation (LHM) strategy, where different layer heights are deliberately combined within the same printed surface through stepwise or gradient stacking designs. The stacking approach enabled spatial control of wettability without altering the base material chemistry. In gradient surfaces, decreasing layer height from 400 µm to 50 µm resulted in a progressive decrease in WCA from ~159° (superhydrophobic) region ~129-132° (hydrophobic region), confirming that layer stacking can generate superhydrophobic-hydrophobic hybrid surfaces with tunable wetting transition behavior. Figure 12 illustrates stacking principle they used.

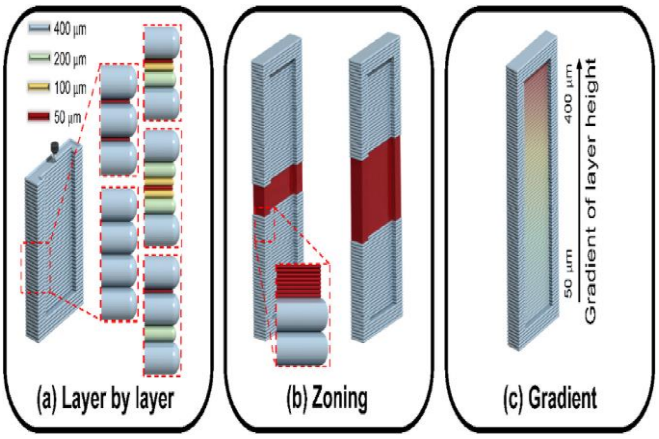

Figure 12. Schematic illustration of 3D printing layer height control techniques: (a) different layer-by-layer heights, (b) rapidly changing layer heights at the middle zone, and (c) continuously changing layer heights

In the work of Atwah et al., layer height was shown to significantly affect surface roughness, porosity, and contact angle across several flexible polymer systems. Their results indicate that increasing layer height generally increases roughness and can enhance apparent hydrophobicity, provided that the resulting surface supports partial wetting rather than complete liquid infiltration. Ayrilmis demonstrated that increasing layer thickness significantly altered the wettability of FDM-fabricated wood/PLA specimens [*Yu et al., 2025*]. The contact angle decreased as layer thickness increased, indicating enhanced wettability and improved liquid spreading on rougher and more porous surfaces. When layer thickness increased from 0.05 mm to 0.30 mm, the contact angle decreased from 75.6° to 64.5°, confirming that rougher surfaces generated by thicker layers promoted water penetration and absorption into micro-pores rather than sustaining droplet repellence. The authors attributed this behavior to the increase in surface roughness and pore density with increasing layer height, which favors liquid infiltration and therefore reduces WCA values. In contrast, other extrusion-printed polymer systems may show the opposite trend, depending on whether the formed microtexture promotes void formation under droplets. However, the influence of layer height is not unidirectional or universally beneficial. Several studies emphasize that excessive roughness or poorly fused layers can increase droplet pinning and promote wetting transitions, particularly when interconnected valleys allow liquid penetration. This complexity is reflected in the work of Buj-Corral et al., who demonstrated that printing temperature, speed and flow rate significantly affect surface roughness and porosity in PLA parts]. Although their primary focus was dimensional accuracy and porosity rather than WCA, the reported decrease in roughness combined with a slight increase in porosity illustrates how process parameters can simultaneously influence multiple surface properties that indirectly govern wettability.

- Influence of extruder width and raster width

Extruder width, raster width and nozzle-related parameters represent another group of variables controlling surface texture geometry. In their analysis, Atwah et al. identified extruder width as a key contributor to roughness and hydrophobicity, as it determines the width of deposited roads and the size of inter-road valleys (Table 4) [*Adabavazeh et al., 2024*]. Similarly, Kingman and Dymond demonstrated that increasing raster width can significantly raise WCA measured perpendicular to the toolpath, an effect attributed to enhanced void formation and more pronounced groove topography.

Table 4. 3D printing parameters in 3D printing of hydrophobic surfaces

Layer Height (LH) mm	Extruder Width (EW) mm	Orientation Angle (O) Degree °
0.15	0.50	0° (first layer)–90° (second layer), 45° (first layer)–135° (second layer)
0.13	0.40	0–90°, 45–135°
0.10	0.30	0–90°, 45–135°

- Influence of surface pattern design and feature spacing

In the study of Amin et al., FDM printed PLA samples showed water contact angles up to 142° with adjusting roughness and sample geometry with printed pyramid shapes [*Yu et al., 2025*]. Increasing distance between pyramid peaks decreased water contact angle. However, this processing involved chemical etching and showed that there are challenges in achieving uniform surface roughness and contact angle. Recently, it has been shown that sample geometry has more significant influence on contact angle than roughness [156]. The microstructure patterns on 3D-printed surfaces influence contact angles. Lohatepanont et al. showed that parametric designs enhance hydrophobicity, while anisotropic systems show lower hydrophobic properties based on water droplet tests. With bioinspired geometry, Rahman et al. printed micro-pillars with contact angles up to 160° and pillar of 0.17mm height and 0.5 mm diameter, 55° reentrant angle, and a spacing of 0.36 mm between pillars [*Oni et al., 2025*]. However, this microstructure is complex and hard to replicate, which limits its application. He et al. constructed superhydrophobic surfaces with the aid of a homemade 3D printer; polydimethylsiloxane ink was used to etch various geometric patterns onto a glass substrate

(Figure 13) [*Sebastian et al., 2018*]. During experimentation, it was discovered that by adjusting the 3D printing parameters such as filament spacing and printing speed, it was possible to achieve superhydrophobic structures.

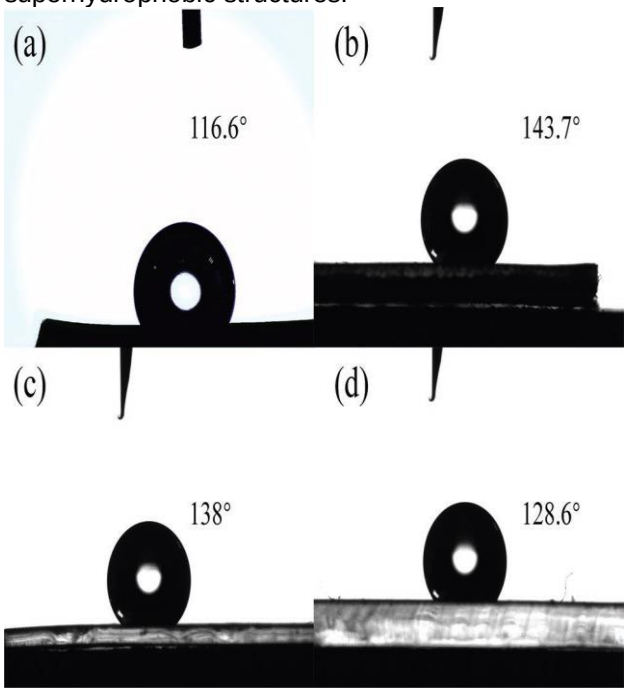

Figure 13. The contact angle of a) polydimethylsiloxane (PDMS) with flat punch micropillars (116.6°). b) PDMS with mushroom-shaped micropillars (143.7°). c) PDMS with suction cupshaped micropillars (138°). d) PDMS with tilted micropillars (128.6°) [158]

Dong et al. introduced a new approach for 3D printing super hydrophobic objects with bulk nanostructure using a specific ink composed of hydrophobic monomers and porogen solvents [*Oni et al., 2025*]. The 3D printed objects exhibited ultralow water adhesion and retained their super hydrophobicity even after wear damage. Chan et al. investigated the self-cleaning behaviour of 3D printed textile fabrics with various printing parameters [126]. They analysed the impact of primary printing parameters, such as infill rate, flow rate, printing temperature, printing speed, and printing acceleration, on the self-cleaning attributes of thermoplastic polyurethane (TPU) fabric. The results highlighted the significant role of flow rate and demonstrated that all parameters influenced the fabric's wettability similarly. These studies highlight the potential of 3D printing for creating functional surfaces with enhanced wettability properties, such as superhydrophobicity, self-cleaning and antiadhesive properties. The optimization of printing parameters and the development of novel fabrication methods contribute to the advancement of surface engineering using 3D printing technology.

- **Influence of flow rate, acceleration, speed and temperature**

While many studies focus on rigid thermoplastics, flexible and textile-like structures provide additional perspectives on parameter-wettability relationships. **Chan et al.** showed that all parameters affected WCA, with **flow rate identified as the most influential variable** . This finding is particularly important because it demonstrates that deposition consistency and filament swelling can dominate surface behavior, even when geometric parameters such as layer height are held constant. Similar conclusions are drawn in the work of **Barrios and Romero**, who identified printing acceleration and flow rate as the most significant factors influencing surface roughness and wettability. Complementary insights are provided by He et al, who explored how printing parameters such as filament spacing and speed influence the wettability of PDMS microstructures with different pillar shapes. Their comparative analysis of flat, mushroom-shaped, suction-cup-shaped, and tilted micropillars revealed contact angles ranging from approximately 116° to 144°, depending on feature morphology. Presented studies collectively reveal the connection between material properties and processing parameters, emphasizing the importance of printing **investigation from different aspects, in order to achieve superhydrophobic WCA**. Table 5 summarizes investigated parameters from influential studies.

Table 5. Influence of printing parameters on WCA

Study	Material	Parameters investigated	Main indications
Neukäufer et al. [140]	PP	LO	Orientation governs anisotropy and droplet suspension
Atwah et al. [137]	TPE/TPU/ TPC	LH, EW, OA	LH, EW, OA control roughness/porosity and CA
Amin et al. [126]	PLA	Feature spacing, etching	Geometry and spacing dominate wetting response
Lohatepanont et al. [143]	Polymer resin	Pattern design, anisotropy	Geometry can dominate over roughness

			alone
Rahman et al. [144]	Bioinspired pillars	LH, diameter, spacing, re-entrant angle	Re-entrant geometry stabilizes partial wetting
Kingman et al. [122]	PLA	LH, RW	Toolpath architecture controls CA
He et al. [145]	Acrylic resin	Spacing, speed pillar shape	WCA depends on micro-feature morphology
Dong et al. [146]	Bulk nanostructured printing	Ink, porogen formulation	Bulk texture improves wear robustness
Chan et al. [112]	TPU textile	Infill, flow, speed, accel., temp.	Flow rate most significant, deposition stability controls wettability
Buj-Corral et al. [142]	PLA	Temp, speed, flow	Roughness down, porosity up
Barrios & Romero [135]	PETG	Acceleration, flow	Kinematic parameters can dominate wettability

4.5 Future outlook in 3d printing application for corrosion protective surfaces

Corrosion protection of steel pipelines represents a vital concern in safeguarding the structural integrity and operational lifespan of assets across critical sectors, including oil and gas, water supply, and civil infrastructure. Although additive manufacturing (AM), particularly 3D printing, has not yet been widely implemented as a direct method for corrosion protection of steel pipes, existing literature suggests that it holds significant promise for advancing protective strategies in several ways [*Sebastian et al., 2018*]. Additive manufacturing facilitates the fabrication of tailor-made coatings and internal linings with controlled thickness, composition, and functional properties. These coatings can be engineered to conform precisely to the pipeline's geometry and surface characteristics, potentially enhancing corrosion resistance through localized optimization of barrier performance and mechanical adhesion. 3D printing technologies enable the integration of intelligent sensing components directly onto pipeline surfaces. The *in situ* fabrication of sensors and probes, capable of detecting parameters such as corrosion rates, localized electrochemical activity or environmental fluctuations, permits real-time monitoring and predictive maintenance. Effective surface preparation is fundamental to the performance of anticorrosive coatings. The ability of 3D printing to create micro- and nano-scale surface textures offers a novel route to passive corrosion protection [160]. Controlled roughness patterns and engineered surface architectures can increase surface area, improve mechanical interlocking of coatings, and reduce wettability, all of which contribute to reduced corrosion susceptibility [*Adabavazeh et al., 2024*]. Pipelines frequently incorporate intricate features such as elbows, joints, and flanges, which are especially prone to corrosion. This includes customized fittings, internal linings, or structural reinforcements that ensure full coverage and mechanical compatibility, thus enhancing the overall efficacy of the corrosion protection system.

CONCLUSIONS

This review has critically examined the persistent challenge of steel pipeline corrosion in diverse soil environments and has identified the significant limitations of conventional protective strategies. The central finding is that 3D printing, particularly through the precise geometric control afforded by material extrusion, offers a novel and powerful pathway for fabricating advanced anti-corrosion surfaces. By enabling the layer-by-layer construction of bio-inspired micro-topographies, such as re-entrant structures and micropillars, 3D printing can produce superhydrophobic surfaces that achieve the Cassie-Baxter state. This mechanism establishes a stable air-liquid interface, or plastron, which serves as a robust physical barrier preventing the contact of corrosive electrolytes (in both acidic and alkaline soils) with the steel substrate. The focus is on the potential of fused deposition modeling (FDM) technique, which is insufficiently investigated for the anticorrosive coatings. The literature review demonstrates that factors such as layer height, orientation, infill patterns and post-processing treatments are main variables in FDM that can be tuned to optimize water contact angle. However, the translation of these promising laboratory findings into viable industrial solutions remains contingent upon overcoming significant challenges, dominantly the poor mechanical stability and long-term service of many current superhydrophobic structures. The potential for 3D printing to create customized protective coatings with anticorrosive properties was presented through superhydrophobic surfaces achieved in state-of-the-art studies. This technology enables a step beyond standardized, passive barrier coatings and toward the development of intelligent and geometrically engineered surfaces for efficient corrosion protection.

5. References

[1] Adabavazeh N, Nikbakht M, Amindoust A, Ali Hassanzadeh-Tabrizi S. The identification and analysis of pivotal factors influencing the corrosion of natural gas pipelines using fuzzy cognitive map. Eng Fail Anal 2024;166:108806. https://doi.org/10.1016/j.engfailanal.2024.108806.

[2] Hussein Farh HM, Ben Seghier MEA, Taiwo R, Zayed T. Analysis and ranking of corrosion causes for water pipelines: a critical review. Npj Clean Water 2023;6:65. https://doi.org/10.1038/s41545-023-00275-5.

[3] Kowalczyk M, Andruszko J, Stefanek P, Mazur R. Failure and Degradation Mechanisms of Steel Pipelines: Analysis and Development of Effective Preventive Strategies. Materials 2024;18:134. https://doi.org/10.3390/ma18010134.

[4] Al-Amiery A, Wan Isahak WNR, Al-Azzawi WK. Sustainable corrosion Inhibitors: A key step towards environmentally responsible corrosion control. Ain Shams Eng J 2024;15:102672. https://doi.org/10.1016/j.asej.2024.102672.

[5] Kassinis C, Aresti L, Koronides M, Christodoulides P, Michailides C, Onoufriou T. A review on the environment's influence on coastal marine steel corrosion and in-situ monitoring. J Mater Sci Mater Eng 2025;20:125. https://doi.org/10.1186/s40712-025-00352-2.

[6] Nuhi M, Abu Seer T, Al Tamimi AM, Modarres M, Seibi A. Reliability Analysis for Degradation Effects of Pitting Corrosion in Carbon Steel Pipes. Procedia Eng 2011;10:1930–5. https://doi.org/10.1016/j.proeng.2011.04.320.

[7] Alsit A, Hamdan H, Al Tahhan AB, Alkhedher M. Stress corrosion cracking under extreme near-neutral GCC conditions, parametric and comparative study using phase field modeling. Heliyon 2023;9:e18544. https://doi.org/10.1016/j.heliyon.2023.e18544.

[8] Bender R, Féron D, Mills D, Ritter S, Bäßler R, Bettge D, et al. Corrosion challenges towards a sustainable society. Mater Corros 2022;73:1730–51. https://doi.org/10.1002/maco.202213140.

[9] Aljibori H, Al-Amiery A, Isahak WNR. Advancements in Corrosion Prevention Techniques. J Bio- Tribo-Corros 2024;10:78. https://doi.org/10.1007/s40735-024-00882-w.

[10] Shamsuddoha M, Islam MM, Aravinthan T, Manalo A, Lau K. Effectiveness of using fibre-reinforced polymer composites for underwater steel pipeline repairs. Compos Struct 2013;100:40–54. https://doi.org/10.1016/j.compstruct.2012.12.019.

[11] Hariharan M, Panikkaveettil Shamsudheen S, Varghese N, Nair AB. Application of UPR in pipeline corrosion: protection and applications. Appl. Unsaturated Polyest. Resins, Elsevier; 2023, p. 309–40. https://doi.org/10.1016/B978-0-323-99466-8.00011-3.

[12] Hu JY, Liu MX, Lan Y, Tao GM, Zhang SS. Challenges and Opportunities for Aging of Fiber-Reinforced Polymer Under Intensive Solar Radiation. Polym Compos 2025:pc.70376. https://doi.org/10.1002/pc.70376.

[13] Mahdavi F, Forsyth M, Tan MYJ. Understanding the effects of applied cathodic protection potential and environmental conditions on the rate of cathodic disbondment of coatings by means of local electrochemical measurements on a multi-electrode array. Prog Org Coat 2017;103:83–92. https://doi.org/10.1016/j.porgcoat.2016.10.020.

[14] Alabtah FG, Mahdi E, Eliyan FF. The use of fiber reinforced polymeric composites in pipelines: A review. Compos Struct 2021;276:114595. https://doi.org/10.1016/j.compstruct.2021.114595.

[15] Alabtah FG, Mahdi E, Eliyan FF, Eltai E, Khraisheh M. Towards the Development of Novel Hybrid Composite Steel Pipes: Electrochemical Evaluation of Fiber-Reinforced Polymer Layered Steel against Corrosion. Polymers 2021;13:3805. https://doi.org/10.3390/polym13213805.

[16] Hill R, Perez AL. New steels and corrosion-resistant alloys. Trends Oil Gas Corros. Res. Technol., Elsevier; 2017, p. 613–26. https://doi.org/10.1016/B978-0-08-101105-8.00026-7.

[17] Reda A, Shahin MA, Sultan IA, Amaechi CV, McKee KK. Necessity and suitability of in-line inspection for corrosion resistant alloy (CRA) clad pipelines. Ships Offshore Struct 2023;18:1360–6. https://doi.org/10.1080/17445302.2022.2117928.

[18] Oni BA, Tomomewo OS, Evro S, Misiani AN, Sanni SE. A review of anticorrosive, superhydrophobic and self-healing properties of coating-composites as corrosion barriers on magnesium alloys: Recent advances, challenges and future directions. J Magnes Alloys 2025;13:2435–69. https://doi.org/10.1016/j.jma.2025.05.013.

[19] Huang Y, Lin G, Yue L, Wang T, Liu X, Zhang B. Superhydrophobic anti-corrosion coatings for metal surfaces: a systematic review from fabrication to performance. New J Chem 2026;50:2132–53. https://doi.org/10.1039/D5NJ04479K.

[20] Tang ZQ, Tian T, Molino PJ, Skvortsov A, Ruan D, Ding J, et al. Recent Advances in Superhydrophobic Materials Development for Maritime Applications. Adv Sci 2024;11:2308152. https://doi.org/10.1002/advs.202308152.

[21] Xiang Q, Zeng J, Qiao B. Multifunctional hydrophobic/superhydrophobic protective coatings for magnesium alloys: A review on material design, protection mechanisms, and engineering applications. J Magnes Alloys 2025:S2213956725003998. https://doi.org/10.1016/j.jma.2025.11.006.

[22] Sebastian D, Yao C-W, Lian I. Mechanical Durability of Engineered Superhydrophobic Surfaces for Anti-Corrosion. Coatings 2018;8:162. https://doi.org/10.3390/coatings8050162.

[23] Ismail A, Elshamy A. Engineering behaviour of soil materials on the corrosion of mild steel. Appl Clay Sci 2009;42:356–62. https://doi.org/10.1016/j.clay.2008.03.003.

[24] Hussein Farh HM, Ben Seghier MEA, Taiwo R, Zayed T. Analysis and ranking of corrosion causes for water pipelines: a critical review. Npj Clean Water 2023;6:65. https://doi.org/10.1038/s41545-023-00275-5.

[25] Park SR, Kim MS, Yoon SM, Yoon SN, Han YJ, Yoon SH, et al. Multifunctional Micro/Nanostructured Interfaces, Fabrication Technologies, Wetting Control, and Future Prospects. Adv Mater Interfaces 2025;12:e00492. https://doi.org/10.1002/admi.202500492.

[26] Mehanna YA, Sadler E, Upton RL, Kempchinsky AG, Lu Y, Crick CR. The challenges, achievements and applications of submersible superhydrophobic materials. Chem Soc Rev 2021;50:6569–612. https://doi.org/10.1039/D0CS01056A.

[27] Sun K, Zhong W, Huang S, He X, Cai W, Ma R, et al. Research Progress on the Corrosion Mechanism and Protection Monitoring of Metal in Power Equipment. Coatings 2025;15:119. https://doi.org/10.3390/coatings15020119.

[28] Manu KC, Madhushree C, Chandini MS, Shree N, Hemanth S, Jeevan TP. Corrosion in Steel Structures: A Review. J Mines Met Fuels

2025:189–98. https://doi.org/10.18311/jmmf/2025/46985.

[29] Alcántara J, Fuente DDL, Chico B, Simancas J, Díaz I, Morcillo M. Marine Atmospheric Corrosion of Carbon Steel: A Review. Materials 2017;10:406. https://doi.org/10.3390/ma10040406.

[30] Zhao L, Liu D, Zhang H, Wang J, Zhang X, Liu S, et al. Study on electrochemical reduction mechanisms of iron oxides in pipe scale in drinking water distribution system. Water Res 2023;231:119597. https://doi.org/10.1016/j.watres.2023.119597.

[31] Rossi S, Pinamonti M, Calovi M. Influence of soil chemical characteristics on corrosion behaviour of galvanized steel. Case Stud Constr Mater 2022;17:e01257. https://doi.org/10.1016/j.cscm.2022.e01257.

[32] Cole IS, Marney D. The science of pipe corrosion: A review of the literature on the corrosion of ferrous metals in soils. Corros Sci 2012;56:5–16. https://doi.org/10.1016/j.corsci.2011.12.001.

[33] Meek AH, Beckett CTS, Carsana M, Ciancio D. Corrosion protection of steel embedded in cement-stabilised rammed earth. Constr Build Mater 2018;187:942–53. https://doi.org/10.1016/j.conbuildmat.2018.07.210.

[34] Amaya-Gómez R, Bastidas-Arteaga E, Muñoz F, Sánchez-Silva M. Statistical Soil Characterization of an Underground Corroded Pipeline Using In-Line Inspections. Metals 2021;11:292. https://doi.org/10.3390/met11020292.

[35] Gadala IM, Alfantazi A. Electrochemical behavior of API-X100 pipeline steel in NS4, near-neutral, and mildly alkaline pH simulated soil solutions. Corros Sci 2014;82:45–57. https://doi.org/10.1016/j.corsci.2013.12.020.

[36] Giron RGP, Chen X, La Plante EC, Gussev MN, Leonard KJ, Sant G. Revealing How Alkali Cations Affect the Surface Reactivity of Stainless Steel in Alkaline Aqueous Environments. ACS Omega 2018;3:14680–8. https://doi.org/10.1021/acsomega.8b02227.

[37] Abd Ghani J, Mohamed Yusop F, Ismail A, Tuan Ismail TNH. Characterization of soil properties influence to the corrosion of the underground pipeline. Mater Today Proc 2024;109:113–9. https://doi.org/10.1016/j.matpr.2024.01.024.

[38] Chen J, Chen Z, Ai Y, Xiao J, Pan D, Li W, et al. Impact of Soil Composition and Electrochemistry on Corrosion of Rock-cut Slope Nets along Railway Lines in China. Sci Rep 2015;5:14939. https://doi.org/10.1038/srep14939.

[39] Linter BR, Burstein GT. Reactions of pipeline steels in carbon dioxide solutions. Corros Sci 1999;41:117–39. https://doi.org/10.1016/S0010-938X(98)00104-8.

[40] Ma F-Y. Corrosive Effects of Chlorides on Metals. In: Bensalah N, editor. Pitting Corros., InTech; 2012. https://doi.org/10.5772/32333.

[41] Liang P, Li X, Du C, Chen X. Stress corrosion cracking of X80 pipeline steel in simulated alkaline soil solution. Mater Des 2009;30:1712–7. https://doi.org/10.1016/j.matdes.2008.07.012.

[42] Liu ZY, Li Q, Cui ZY, Wu W, Li Z, Du CW, et al. Field experiment of stress corrosion cracking behavior of high strength pipeline steels in typical soil environments. Constr Build Mater 2017;148:131–9. https://doi.org/10.1016/j.conbuildmat.2017.05.058.

[43] Ryakhovskikh IV, Bogdanov RI, Ignatenko VE. Intergranular stress corrosion cracking of steel gas pipelines in weak alkaline soil electrolytes. Eng Fail Anal 2018;94:87–95. https://doi.org/10.1016/j.engfailanal.2018.07.036.

[44] Tran Thi Thuy T, Kannoorpatti K, Padovan A, Thennadil S. Effect of Alkaline Artificial Seawater Environment on the Corrosion Behaviour of Duplex Stainless Steel 2205. Appl Sci 2020;10:5043. https://doi.org/10.3390/app10155043.

[45] Wasim M, Shoaib S, Mubarak NM, Inamuddin, Asiri AM. Factors influencing corrosion of metal pipes in soils. Environ Chem Lett 2018;16:861–79. https://doi.org/10.1007/s10311-018-0731-x.

[46] Du CW, Li XG, Liang P, Liu ZY, Jia GF, Cheng YF. Effects of Microstructure on Corrosion of X70 Pipe Steel in an Alkaline Soil. J Mater Eng Perform 2009;18:216–20. https://doi.org/10.1007/s11665-008-9280-y.

[47] Qi G, Qin X, Xie J, Han P, He B. Electrochemical corrosion behaviour of four low-carbon steels in saline soil. RSC Adv 2022;12:20929–45. https://doi.org/10.1039/D2RA03200G.

[48] Wu YH, Liu TM, Luo SX, Sun C. Corrosion characteristics of Q235 steel in simulated Yingtan soil solutions. Mater Werkst 2010;41:142–6. https://doi.org/10.1002/mawe.201000559.

[49] Liu TM, Wu YH, Luo SX, Sun C. Effect of soil compositions on the electrochemical corrosion behavior of carbon steel in simulated soil solution. Mater Werkst 2010;41:228–33. https://doi.org/10.1002/mawe.201000578.

[50] Noor E, Al-Moubaraki A, Al-Masoudi D, Chafiq M, Chaouiki A, Ko Y. Corrosion Behavior of Carbon Steel X36 in Solutions of Soils Collected from Different Areas Linked to the Main Pipe Network of a Water Distribution System in Jeddah City. Metals 2023;13:670. https://doi.org/10.3390/met13040670.

[51] Benmoussa A, Hadjel M, Traisnel M. Corrosion behavior of API 5L X-60 pipeline steel exposed to near-neutral pH soil simulating solution. Mater Corros 2006;57:771–7. https://doi.org/10.1002/maco.200503964.

[52] Popoola LT. Progress on pharmaceutical drugs, plant extracts and ionic liquids as corrosion inhibitors. Heliyon 2019;5:e01143. https://doi.org/10.1016/j.heliyon.2019.e01143.

[53] Alhajji J. Pitting corrosion of stainless steels in acidic environment. Br Corros J 1997;32:291–6. https://doi.org/10.1179/bcj.1997.32.4.291.

[54] Mohammed HK, Jafar SA, Humadi JI, Sehgal S, Saxena KK, Abdullah GH, et al. Investigation of carbon steel corrosion rate in different acidic environments. Mater Today Proc 2023:S2214785323018643. https://doi.org/10.1016/j.matpr.2023.03.792.

[55] Xiang Y, Li C, Long Z, Guan C, Wang W, Hesitao W. Electrochemical behavior of valve steel in a CO2/sulfurous acid solution. Electrochimica Acta 2017;258:909–18. https://doi.org/10.1016/j.electacta.2017.11.141.

[56] Abd El-Lateef HM, Mohamed IMA, Zhu J-H, Khalaf MM. An efficient synthesis of electrospun TiO2-nanofibers/Schiff base phenylalanine composite and its inhibition behavior for C-steel corrosion in acidic chloride environments. J Taiwan Inst Chem Eng 2020;112:306–21. https://doi.org/10.1016/j.jtice.2020.06.002.

[57] Ramezanzadeh B, Haeri Z, Ramezanzadeh M. A facile route of making silica nanoparticles-covered graphene oxide nanohybrids (SiO2-GO); fabrication of SiO2-GO/epoxy composite coating with superior barrier and corrosion protection performance. Chem Eng J 2016;303:511–28. https://doi.org/10.1016/j.cej.2016.06.028.

[58] Hu C, Li Y, Zhang N, Ding Y. Synthesis and characterization of a poly(o-anisidine)–SiC composite and its application for corrosion protection of steel. RSC Adv 2017;7:11732–42. https://doi.org/10.1039/C6RA27343B.

[59] Morozov Y, Calado LM, Shakoor RA, Raj R, Kahraman R, Taryba MG, et al. Epoxy coatings modified with a new cerium phosphate inhibitor

for smart corrosion protection of steel. Corros Sci 2019;159:108128. https://doi.org/10.1016/j.corsci.2019.108128.

[60] Zhang J, Zhang W, Wei L, Pu L, Liu J, Liu H, et al. Alternating Multilayer Structural Epoxy Composite Coating for Corrosion Protection of Steel. Macromol Mater Eng 2019;304:1900374. https://doi.org/10.1002/mame.201900374.

[61] Arabpour A, Shockravi A, Rezania H, Farahati R. Investigation of anticorrosive properties of novel silane-functionalized polyamide/GO nanocomposite as steel coatings. Surf Interfaces 2020;18:100453. https://doi.org/10.1016/j.surfin.2020.100453.

[62] Lei Y, Qiu Z, Tan N, Du H, Li D, Liu J, et al. Polyaniline/CeO2 nanocomposites as corrosion inhibitors for improving the corrosive performance of epoxy coating on carbon steel in 3.5% NaCl solution. Prog Org Coat 2020;139:105430. https://doi.org/10.1016/j.porgcoat.2019.105430.

[63] Liu B, Du C, Li X, Wang D, Xu J, Sun C, et al. Effect of Alternating Current and Cathodic Protection on Corrosion of X80 Steel in Alkaline Soil. J Mater Eng Perform 2022;31:1769–80. https://doi.org/10.1007/s11665-021-06309-8.

[64] Kwak J, Hong S-H, Jung S-M, Kim K-S, Jeong C-G, Lee B-J, et al. Influence of magnesium addition in Al–Zn–Si coatings on sacrificial corrosion behavior and corrosion product formation on steel substrates. J Mater Res Technol 2026;40:2584–93. https://doi.org/10.1016/j.jmrt.2025.12.071.

[65] Permeh S, Lau K. Corrosion of galvanized steel in alkaline solution associated with sulfate and chloride ions. Constr Build Mater 2023;392:131889. https://doi.org/10.1016/j.conbuildmat.2023.131889.

[66] Roventi G, Bellezze T, Giuliani G, Conti C. Corrosion resistance of galvanized steel reinforcements in carbonated concrete: effect of wet–dry cycles in tap water and in chloride solution on the passivating layer. Cem Concr Res 2014;65:76–84. https://doi.org/10.1016/j.cemconres.2014.07.014.

[67] Ramezanzadeh B, Haeri Z, Ramezanzadeh M. A facile route of making silica nanoparticles-covered graphene oxide nanohybrids (SiO2-GO); fabrication of SiO2-GO/epoxy composite coating with superior barrier and corrosion protection performance. Chem Eng J 2016;303:511–28. https://doi.org/10.1016/j.cej.2016.06.028.

[68] Morozov Y, Calado LM, Shakoor RA, Raj R, Kahraman R, Taryba MG, et al. Epoxy coatings modified with a new cerium phosphate inhibitor for smart corrosion protection of steel. Corros Sci 2019;159:108128. https://doi.org/10.1016/j.corsci.2019.108128.

[69] Anjum A, Garg R, Kashif Mohd, Eddy NO. High-performance polymer nanocomposite coatings for enhanced and sustainable corrosion protection. Inorg Chem Commun 2025;178:114411. https://doi.org/10.1016/j.inoche.2025.114411.

[70] Arabpour A, Shockravi A, Rezania H, Farahati R. Investigation of anticorrosive properties of novel silane-functionalized polyamide/GO nanocomposite as steel coatings. Surf Interfaces 2020;18:100453. https://doi.org/10.1016/j.surfin.2020.100453.

[71] Guan H, Lv F, Li D, Wang Y, Lu X, Bian D. Anti-corrosion property of multilayer Ti3C2Tx reinforced chemically bonded silicate ceramic coatings in salt, alkaline and acid environments. Ceram Int 2023;49:38961–72. https://doi.org/10.1016/j.ceramint.2023.09.232.

[72] Goswami RN, Mourya P, Saini R, Pandey A, Konathala L, Ray A, et al. Polyaniline-wrapped h-boron nitride nanosheets as anticorrosive filler in

epoxy coatings for substantially enhanced protection of mild steel. J Ind Eng Chem 2024;140:285–97. https://doi.org/10.1016/j.jiec.2024.05.048.

[73] Shaily, Zafar F, Ghosal A, Alam M, Naaz H, Fatma T, et al. In situ nano silver-imbosed cardanol-based polyurethane nanomaterial as protective coating of mild steel: Synthesis, characterization, antibacterial and anticorrosive analysis. J Mol Struct 2025;1348:143333. https://doi.org/10.1016/j.molstruc.2025.143333.

[74] Jahan A, Masood S, Zafar F, Shaily, Rizvi SA, Alam M, et al. Development of cardanol based antibacterial and anticorrosive bio-polyurea-epoxy composite coating for mild steel surface. Prog Org Coat 2024;189:108273. https://doi.org/10.1016/j.porgcoat.2024.108273.

[75] Liu Z, Shu B, Liu Z, Li X, Wu T, Xiang Z, et al. Mussel-inspired synergistic anticorrosive coatings for steel substrate prepared basing on fully bio-based epoxy resin and biomass modified graphene nanoparticles. Colloids Surf Physicochem Eng Asp 2024;693:134038. https://doi.org/10.1016/j.colsurfa.2024.134038.

[76] Dagdag O, El Harfi A, El Gana L, S. Safi Z, Guo L, Berisha A, et al. Designing of phosphorous based highly functional dendrimeric macromolecular resin as an effective coating material for carbon steel in NaCl : Computational and experimental studies. J Appl Polym Sci 2021;138:49673. https://doi.org/10.1002/app.49673.

[77] Oni BA, Tomomewo OS, Evro S, Misiani AN, Sanni SE. A review of anticorrosive, superhydrophobic and self-healing properties of coating-composites as corrosion barriers on magnesium alloys: Recent advances, challenges and future directions. J Magnes Alloys 2025;13:2435–69. https://doi.org/10.1016/j.jma.2025.05.013.

[78] De Leon ACC, Pernites RB, Advincula RC. Superhydrophobic Colloidally Textured Polythiophene Film as Superior Anticorrosion Coating. ACS Appl Mater Interfaces 2012;4:3169–76. https://doi.org/10.1021/am300513e.

[79] Han X, You Z, Liu Y, Ma R, Fan Y, Du A, et al. Preparation of ETFE-ZrO2 superhydrophobic composite coating on Q345 steel surface and its performance study. Prog Org Coat 2025;200:108977. https://doi.org/10.1016/j.porgcoat.2024.108977.

[80] Braga AVDC, Do Lago DCB, Pimenta AR, De Senna LF. The influence of heat treatment of inorganic conversion coatings produced by sol-gel dip coating on the anticorrosive properties of alumina films deposited on steel substrate – Part I: Single conversion coatings. Surf Coat Technol 2019;372:190–200. https://doi.org/10.1016/j.surfcoat.2019.05.040.

[81] Vigilianska N, Iantsevitch C, Tsymbalista T, Burlachenko O, Grishchenko O, Gudymenko O, et al. Formation of Coatings Containing Cr2AlC MAX Phase During Plasma Spraying of Mixture of Cr3C2+Al Powders. Coatings 2024;14:1584. https://doi.org/10.3390/coatings14121584.

[82] Zhou Y, Yu Y, Guo W, Xing F, Guo M. Development of inorganic anticorrosive coatings for steel bars: Corrosion resistance testing and design. Cem Concr Compos 2024;152:105612. https://doi.org/10.1016/j.cemconcomp.2024.105612.

[83] Yin S, Yang H, Dong Y, Qu C, Liu J, Guo T, et al. Environmentally favorable magnesium phosphate anti-corrosive coating on carbon steel and protective mechanisms. Sci Rep 2021;11:197. https://doi.org/10.1038/s41598-020-79613-3.

[84] Udoh II, Dam-Johansen K. Chitosan-capped mesoporous silica nano/microcontainers for waterborne epoxy coating: Implications of size

and textural properties modulated by synthesis route. Appl Mater Today 2025;42:102539. https://doi.org/10.1016/j.apmt.2024.102539.

[85] Yue P, Zhang M, Zhao T, Liu P, Peng F, Yang L. Eco-friendly epoxidized Eucommia ulmoides gum based composite coating with enhanced super-hydrophobicity and corrosion resistance properties. Ind Crops Prod 2024;214:118523. https://doi.org/10.1016/j.indcrop.2024.118523.

[86] Udoh II, Ekerenam OO, Daniel EF, Ikeuba AI, Njoku DI, Kolawole SK, et al. Developments in anticorrosive organic coatings modulated by nano/microcontainers with porous matrices. Adv Colloid Interface Sci 2024;330:103209. https://doi.org/10.1016/j.cis.2024.103209.

[87] Karattu Veedu K, Banyangala M, Peringattu Kalarikkal T, Balappa Somappa S, Karimbintherikkal Gopalan N. Green approach in anticorrosive coating for steel protection by Gliricidia sepium leaf extract and silica hybrid. J Mol Liq 2023;369:120967. https://doi.org/10.1016/j.molliq.2022.120967.

[88] Rajimol PR, Ulaeto SB, Puthiyamadam A, Neethu S, Rajan TPD, Radhakrishnan KV, et al. Smart anticorrosive and antimicrobial multifunctional epoxy coating using bergenin and malabaricone C bio-nanocomposite dispersoids on mild steel and aluminium-6061 alloy. Prog Org Coat 2022;169:106924. https://doi.org/10.1016/j.porgcoat.2022.106924.

[89] Radhamani A, Lau HC, Ramakrishna S. Nanocomposite coatings on steel for enhancing the corrosion resistance: A review. J Compos Mater 2020;54:681–701. https://doi.org/10.1177/0021998319857807.

[90] Principles of Corrosion Engineering and Corrosion Control. Elsevier; 2006. https://doi.org/10.1016/B978-0-7506-5924-6.X5000-4.

[91] Varela F, Tan MYJ, Forsyth M. Understanding the effectiveness of cathodic protection under disbonded coatings. Electrochimica Acta 2015;186:377–90. https://doi.org/10.1016/j.electacta.2015.10.171.

[92] Mayer-Trzaskowska P, Ferraris M, Perero S, Robakowska M. The Influence of the Addition of Rubber Waste on the Properties of Polyurethane Coatings Subjected to Aging Processes. Coatings 2025;15:677. https://doi.org/10.3390/coatings15060677.

[93] Smoleń J, Olesik P, Nowacki B, Godzierz M, Kurtyka K, Chaber P, et al. The influence of UV radiation on the properties of GFRP laminates in underwater conditions. Sci Rep 2024;14:7446. https://doi.org/10.1038/s41598-024-57999-8.

[94] Firoozi A, Firoozi A, Oyejobi DO, Avudaiappan S, Flores E. Enhanced durability and environmental sustainability in marine infrastructure: Innovations in anti-corrosive coating technologies. Results Eng 2025;26:105144. https://doi.org/10.1016/j.rineng.2025.105144.

[95] Zeng L, Liu M, Wu L, Zhou C, Abi E. Erosion characteristics of viscoelastic anticorrosive coatings for steel structures under sand flow. Constr Build Mater 2020;258:120360. https://doi.org/10.1016/j.conbuildmat.2020.120360.

[96] Hlavackova V, Koutnik P, Liskova K, Cmelik J, Riha J, Stoulil J, et al. Microbially Influenced Corrosion in Epoxy-Ceramic Coated Carbon-Steel Cooler. Mater Corros 2025;76:1154–68. https://doi.org/10.1002/maco.202414671.

[97] Km S, Praveen BM, Devendra BK. A review on corrosion inhibitors: Types, mechanisms, electrochemical analysis, corrosion rate and efficiency of corrosion inhibitors on mild steel in an acidic environment. Results Surf Interfaces 2024;16:100258. https://doi.org/10.1016/j.rsurfi.2024.100258.

[98] Zhao Y, Yang Q, Khalaf AH, Lin B, Tang J. Long-Term Anti-Corrosion Performance of Ultra-High Content Inhibitor Loaded Gel-Epoxy Solid

Inhibitor with Temperature-Responisve Effect. Appl Sci 2025;15:3964. https://doi.org/10.3390/app15073964.

[99] Ouarga A, Zirari T, Fashu S, Lahcini M, Ben Youcef H, Trabadelo V. Corrosion of iron and nickel based alloys in sulphuric acid: Challenges and prevention strategies. J Mater Res Technol 2023;26:5105–25. https://doi.org/10.1016/j.jmrt.2023.08.198.

[100] R. Holla B, Mahesh R, Manjunath HR, Anjanapura VR. Plant extracts as green corrosion inhibitors for different kinds of steel: A review. Heliyon 2024;10:e33748. https://doi.org/10.1016/j.heliyon.2024.e33748.

[101] Houda SNE, Amel B. Eco-friendly green inhibitor for corrosion protection of API 5L X60 carbon steel in sulfuric acid solution. J Taiwan Inst Chem Eng 2025;173:106161. https://doi.org/10.1016/j.jtice.2025.106161.

[102] Mungwari CP, Obadele BA, King'ondu CK. Phytochemicals as green and sustainable corrosion inhibitors for mild steel and aluminium: Review. Results Surf Interfaces 2025;18:100374. https://doi.org/10.1016/j.rsurfi.2024.100374.

[103] Verma C, Alameri A, Barsoum I, Alfantazi A. Review on corrosion-related aspects of metallic alloys additive manufactured with laser powder bed-fusion (LPBF) technology. Prog Addit Manuf 2025;10:3195–223. https://doi.org/10.1007/s40964-024-00810-x.

[104] Mohammed A, Jiménez A, Bidare P, Elshaer A, Memic A, Hassanin H, et al. Review on Engineering of Bone Scaffolds Using Conventional and Additive Manufacturing Technologies. 3D Print Addit Manuf 2024;11:1418–40. https://doi.org/10.1089/3dp.2022.0360.

[105] Schuhmann D, Rupp M, Merkel M, Harrison DK. Additive vs. Conventional Manufacturing of Metal Components: Selection of the Manufacturing Process Using the AHP Method. Processes 2022;10:1617. https://doi.org/10.3390/pr10081617.

[106] Singh T, Kumar S, Sehgal S. 3D printing of engineering materials: A state of the art review. Mater Today Proc 2020;28:1927–31. https://doi.org/10.1016/j.matpr.2020.05.334.

[107] Mohammed A, Jiménez A, Bidare P, Elshaer A, Memic A, Hassanin H, et al. Review on Engineering of Bone Scaffolds Using Conventional and Additive Manufacturing Technologies. 3D Print Addit Manuf 2023:3dp.2022.0360. https://doi.org/10.1089/3dp.2022.0360.

[108] Schuhmann D, Rupp M, Merkel M, Harrison DK. Additive vs. Conventional Manufacturing of Metal Components: Selection of the Manufacturing Process Using the AHP Method. Processes 2022;10:1617. https://doi.org/10.3390/pr10081617.

[109] Egan PF. Design for Additive Manufacturing: Recent Innovations and Future Directions. Designs 2023;7:83. https://doi.org/10.3390/designs7040083.

[110] Jung S, Kara LB, Nie Z, Simpson TW, Whitefoot KS. Is Additive Manufacturing an Environmentally and Economically Preferred Alternative for Mass Production? Environ Sci Technol 2023;57:6373–86. https://doi.org/10.1021/acs.est.2c04927.

[111] Mirzaali MJ, Moosabeiki V, Rajaai SM, Zhou J, Zadpoor AA. Additive Manufacturing of Biomaterials—Design Principles and Their Implementation. Materials 2022;15:5457. https://doi.org/10.3390/ma15155457.

[112] Gibson I, Rosen D, Stucker B. Additive Manufacturing Technologies: 3D Printing, Rapid Prototyping, and Direct Digital Manufacturing. New York, NY: Springer New York; 2015. https://doi.org/10.1007/978-1-4939-2113-3.

[113] Cheng M, Deivanayagam R, Shahbazian-Yassar R. 3D Printing of Electrochemical Energy Storage Devices: A Review of Printing Techniques and Electrode/Electrolyte Architectures. Batter Supercaps 2020;3:130–46. https://doi.org/10.1002/batt.201900130.

[114] Khosravani MR, Reinicke T. On the environmental impacts of 3D printing technology. Appl Mater Today 2020;20:100689. https://doi.org/10.1016/j.apmt.2020.100689.

[115] Hüner B, Kıstı M, Uysal S, Uzgören İN, Özdoğan E, Süzen YO, et al. An Overview of Various Additive Manufacturing Technologies and Materials for Electrochemical Energy Conversion Applications. ACS Omega 2022;7:40638–58. https://doi.org/10.1021/acsomega.2c05096.

[116] Mazzanti V, Malagutti L, Mollica F. FDM 3D Printing of Polymers Containing Natural Fillers: A Review of their Mechanical Properties. Polymers 2019;11:1094. https://doi.org/10.3390/polym11071094.

[117] Mogan J, Harun WSW, Kadirgama K, Ramasamy D, Foudzi FM, Sulong AB, et al. Fused Deposition Modelling of Polymer Composite: A Progress. Polymers 2022;15:28. https://doi.org/10.3390/polym15010028.

[118] Mantada P, Mendricky R, Safka J. PARAMETERS INFLUENCING THE PRECISION OF VARIOUS 3D PRINTING TECHNOLOGIES. MM Sci J 2017;2017:2004–12. https://doi.org/10.17973/MMSJ.2017_12_201776.

[119] Shams H, Basit K, Khan MA, Mansoor A, Saleem S. Scalable wear resistant 3D printed slippery liquid infused porous surfaces (SLIPS). Addit Manuf 2021;48:102379. https://doi.org/10.1016/j.addma.2021.102379.

[120] Mogan J, Harun WSW, Kadirgama K, Ramasamy D, Foudzi FM, Sulong AB, et al. Fused Deposition Modelling of Polymer Composite: A Progress. Polymers 2022;15:28. https://doi.org/10.3390/polym15010028.

[121] Nukala PK, Palekar S, Solanki N, Fu Y, Patki M, Shohatee AA, et al. Investigating the Application of FDM 3D Printing Pattern in Preparation of Patient-Tailored Dosage Forms. J 3D Print Med 2019;3:23–37. https://doi.org/10.2217/3dp-2018-0028.

[122] Tan DK, Maniruzzaman M, Nokhodchi A. Advanced Pharmaceutical Applications of Hot-Melt Extrusion Coupled with Fused Deposition Modelling (FDM) 3D Printing for Personalised Drug Delivery. Pharmaceutics 2018;10:203. https://doi.org/10.3390/pharmaceutics10040203.

[123] Roudný P, Syrový T. Thermal conductive composites for FDM 3D printing: A review, opportunities and obstacles, future directions. J Manuf Process 2022;83:667–77. https://doi.org/10.1016/j.jmapro.2022.09.026.

[124] Jayanth N, Senthil P, Mallikarjuna B. Experimental investigation on the application of FDM 3D printed conductive ABS-CB composite in EMI shielding. Radiat Phys Chem 2022;198:110263. https://doi.org/10.1016/j.radphyschem.2022.110263.

[125] Atwah AA, Khan MA. Influence of microscopic features on the self-cleaning ability of textile fabrics. Text Res J 2023;93:450–67. https://doi.org/10.1177/00405175211069881.

.

[129] Yang Q, Li X, Xue Y, Peng H, Bai Y, Li W, et al. Recent advances in fluorinated superhydrophobic materials: Preparation and diverse applications. Chem Eng J 2025;523:168236. https://doi.org/10.1016/j.cej.2025.168236.

[130] Wang Y, Xu Y, Zhang F, Chen X, Lu L, Shen C, et al. Polymers on performance optimization of superhydrophobic cementitious material. Mater

Today Commun 2025;49:113900. https://doi.org/10.1016/j.mtcomm.2025.113900.

[131] Sung J, So H. 3D printing-assisted fabrication of microgrid patterns for flexible antiadhesive polymer surfaces. Surf Interfaces 2021;23:100935. https://doi.org/10.1016/j.surfin.2021.100935.

[132] Tezel T, Kovan V, Ozenc M. Enhancing mechanical properties of 3D-printed PLA composites via topology optimization and nickel coating. Polym-Plast Technol Mater 2025;64:1798–805. https://doi.org/10.1080/25740881.2025.2480844.

[133] Das S, Kumar S, Samal SK, Mohanty S, Nayak SK. A Review on Superhydrophobic Polymer Nanocoatings: Recent Development and Applications. Ind Eng Chem Res 2018;57:2727–45. https://doi.org/10.1021/acs.iecr.7b04887.

[134] Nadi I, Bouanis M, Nohair K, Nyassi A, Zarrouk A, Jama C, et al. Elaboration and corrosion resistance of self-assembled 2,5-bis(4-pyridyl)−1,3,4-oxadiazole film on carbon steel: Surface characterisations, electrochemical assessments and surface pre-treatment effect. Mater Today Commun 2023;35:106382. https://doi.org/10.1016/j.mtcomm.2023.106382.

[135] Amjad M, Nguir M, Ma X, Wen D. Superhydrophobic 3D-printed microstructures: applications, challenges, and prospects. Prog Addit Manuf 2025;10:7337–64. https://doi.org/10.1007/s40964-025-01155-9.

[136] Kingman J, Dymond MK. Fused filament fabrication and water contact angle anisotropy: The effect of layer height and raster width on the wettability of 3D printed polylactic acid parts. Chem Data Collect 2022;40:100884. https://doi.org/10.1016/j.cdc.2022.100884.

[138] Lee K-M, Park H, Kim J, Chun D-M. Fabrication of a superhydrophobic surface using a fused deposition modeling (FDM) 3D printer with poly lactic acid (PLA) filament and dip coating with silica nanoparticles. Appl Surf Sci 2019;467–468:979–91. https://doi.org/10.1016/j.apsusc.2018.10.205.

[139] Zhao W, Zhan Y, Li W, Hao S, Amirfazli A. Application of 3D printing for fabrication of superhydrophobic surfaces with reversible wettability. RSC Adv 2024;14:17684–95. https://doi.org/10.1039/D4RA02742F.

[140] Zhan Y, Pang Z, Tan G. Optically/thermally dual-responsive shape memory superhydrophobic surfaces with advanced multi-functionalities. Compos Part Appl Sci Manuf 2025;192:108812. https://doi.org/10.1016/j.compositesa.2025.108812.

[148] Manderfeld E, Vogler L, Rosenhahn A. Fouling Inhibition by Replenishable Plastrons on Microstructured, Superhydrophobic Carbon-Silicone Composite Coatings. Adv Mater Interfaces 2024;11:2300964. https://doi.org/10.1002/admi.202300964.

[149] Barrios JM, Romero PE. Improvement of Surface Roughness and Hydrophobicity in PETG Parts Manufactured via Fused Deposition Modeling (FDM): An Application in 3D Printed Self–Cleaning Parts. Materials 2019;12:2499. https://doi.org/10.3390/ma12152499.

[150] Jin Y, Li H, He Y, Fu J. Quantitative analysis of surface profile in fused deposition modelling. Addit Manuf 2015;8:142–8. https://doi.org/10.1016/j.addma.2015.10.001.

[151] Kang B, Sung J, So H. Realization of Superhydrophobic Surfaces Based on Three-Dimensional Printing Technology. Int J Precis Eng Manuf-Green Technol 2021;8:47–55. https://doi.org/10.1007/s40684-019-00163-9.

[152] Neukäufer J, Seyfang B, Grützner T. Investigation of Contact Angles and Surface Morphology of 3D-Printed Materials. Ind Eng Chem Res 2020;59:6761–6. https://doi.org/10.1021/acs.iecr.0c00430.

[153] Sung J, Choi Y, So H. Fabrication of functional surfaces using layer height method in material extrusion type 3D printing. J Mater Res Technol 2024;33:749–57. https://doi.org/10.1016/j.jmrt.2024.09.050.

[154] Ayrilmis N. Effect of layer thickness on surface properties of 3D printed materials produced from wood flour/PLA filament. Polym Test 2018;71:163–6. https://doi.org/10.1016/j.polymertesting.2018.09.009.

[155] Buj-Corral I, Bagheri A, Sivatte-Adroer M. Effect of Printing Parameters on Dimensional Error, Surface Roughness and Porosity of FFF Printed Parts with Grid Structure. Polymers 2021;13:1213. https://doi.org/10.3390/polym13081213.

[156] Lohatepanont M, Chen M, Mendoza Nova LC, Murray J-T, Merchan-Merchan W. Exploring Microstructure Patterns: Influence on Hydrophobic Properties of 3D-Printed Surfaces. Micro 2024;4:442–59. https://doi.org/10.3390/micro4030028.

[157] Rahman MMT, Joyee EB. 3D Printed Bioinspired Hierarchical Surface Structure With Tunable Wettability. Vol. 1 Addit. Manuf. Adv. Mater. Manuf. Biomanufacturing Life Cycle Eng., New Brunswick, New Jersey, USA: American Society of Mechanical Engineers; 2023, p. V001T03A012. https://doi.org/10.1115/MSEC2023-104516.

[158] He Q, Zhao Z, Zhang H, Duan J, Zhang N, Cui K, et al. Bioinspired Adhesive Manufactured by Projection Microstereolithography 3D Printing Technology and Its Application. Adv Mater Interfaces 2023;10:2202465. https://doi.org/10.1002/admi.202202465.

[159] Dong Z, Vuckovac M, Cui W, Zhou Q, Ras RHA, Levkin PA. 3D Printing of Superhydrophobic Objects with Bulk Nanostructure. Adv Mater 2021;33:2106068. https://doi.org/10.1002/adma.202106068.

[160] Jiang X, Liu J, Wang Y, Ding Z, Yao M, Ji L, et al. Optimization of micro/nano ceramic 3D-printing process for scale-textured surfaces for enhanced tribological performance. Addit Manuf Front 2025;4:200244. https://doi.org/10.1016/j.amf.2025.200244.

[161] Afshar-Mohajer M, Yang X, Long R, Zou M. 3D printing of micro/nano-hierarchical structures with various structural stiffness for controlling friction and deformation. Addit Manuf 2023;62:103368. https://doi.org/10.1016/j.addma.2022.103368.

[162] Yu Z, Sha P, Yang Y, Yang K, Guo B, Mu Z, et al. Research on the preparation and corrosion resistance of integrated NiTi alloy bionic superhydrophobic corrosion-resistant surface based on additive manufacturing technology. Appl Surf Sci 2025;685:162048. https://doi.org/10.1016/j.apsusc.2024.162048.